PLOS Pathogens

RESEARCH ARTICLE

Polo-like kinase 1 regulates growth in juvenile *Fasciola hepatica*

Paul McCusker[1☯*], Nathan G. Clarke[1☯], Rebecca Armstrong[1], Duncan Wells[1], Emily Robb[1], Paul McVeigh[1], Andreas Krasky[2], John Harrington[3], Paul M. Selzer[2], Nikki J. Marks[1], Aaron G. Maule[1*]

1 Understanding Health & Disease, School of Biological Sciences, Queen's University Belfast, Belfast, United Kingdom, **2** Boehringer Ingelheim Animal Health, Ingelheim am Rhein, Germany, **3** Boehringer Ingelheim Animal Health, Athens, Georgia, United States of America

☯ These authors contributed equally to this work.
* pmccusker09@qub.ac.uk (PM); a.maule@qub.ac.uk (AGM)

Check for updates

OPEN ACCESS

Citation: McCusker P, Clarke NG, Armstrong R, Wells D, Robb E, McVeigh P, et al. (2025) Polo-like kinase 1 regulates growth in juvenile *Fasciola hepatica*. PLoS Pathog 21(12): e1013406. https://doi.org/10.1371/journal.ppat.1013406

Editor: Mostafa Zamanian, University of Wisconsin-Madison, UNITED STATES OF AMERICA

Received: July 23, 2025

Accepted: November 19, 2025

Published: December 2, 2025

Copyright: © 2025 McCusker et al. This is an open access article distributed under the terms of the Creative Commons Attribution License, which permits unrestricted use, distribution, and reproduction in any medium, provided the original author and source are credited.

Data availability statement: The data that support the findings of this study are available within the article, its supplementary materials (S3, S9 and S11 Tables) and from the European Nucleotide Archive at https://www.ebi.ac.uk/ena/browser/view/PRJEB85227, accession

Abstract

Fasciola sp. (liver fluke) are parasitic flatworms that impose a significant burden on the agri-food industry and human health. Immature worms can cause severe damage to the liver as they migrate towards the bile ducts, and yet there is only a single drug to treat this pathogenic life stage, driving the need to identify targets for novel flukicides. Given their crucial role in the growth/development of immature *Fasciola hepatica*, neoblast-like stem cells are an attractive source of new flukicide targets. Kinases are a hugely diverse group of phosphorylating enzymes with key roles in almost all cellular processes. Kinase dysregulation can result in the development of cancerous cells/tissues, linking many to cell cycle-associated proliferation and growth. Here, we annotate the *F. hepatica* kinome, identifying 271 putative protein kinases, representing around 1.6% of predicted *F. hepatica* protein-coding genes with family proportions similar to those of other parasitic flatworms. Many of these kinases, such as polo-like kinase 1 (*fhplk1*), are upregulated in immature worms undergoing rapid growth and development, a process underpinned by the proliferation of neoblast-like stem cells. RNA interference (RNAi)-mediated silencing of *fhplk1* in juvenile liver fluke reduced growth and cell proliferation, suggesting a conserved role within the cell-cycle; the cessation of stem cell proliferation persisted for at least a week following *fhplk1*-RNAi. A PLK inhibitor (BI 2536) was shown to phenocopy the *fhplk1*-RNAi phenotype in a dose-dependent manner, supporting the feasibility of targeting *F. hepatica* neoblast-like cells through kinase inhibitors. Transcriptomic analysis of *fhplk1*-RNAi juveniles revealed 946 downregulated genes, principally associated with the cell cycle or ribosomes. Over 80 of these downregulated genes were also downregulated following juvenile *F. hepatica* irradiation, supporting roles for these kinases in neoblast-like stem cells, and marking them as putative targets for control. Among the 1244 upregulated genes in *fhplk1*-RNAi juvenile worms were many

number PRJEB85227 and https://www.ebi.ac.uk/ena/browser/view/PRJEB85228, accession number PRJEB85228.

Funding: This work was supported by funding from the Biotechnology and Biological Sciences Research Council (https://www.ukri.org/councils/bbsrc/) and Boehringer Ingelheim Animal Health (Companion Animals, House Pets and Equines | Boehringer Ingelheim (https://www.boehringer-ingelheim.com)) through industrial partnership grant BB/T002727/1 awarded to AGM and NJM. Additional funding came from a Department for the Economy, Northern Ireland (https://www.economy-ni.gov.uk/) PhD studentship awarded to NGC and DW and a Department for Agriculture, Environment and Rural Affairs, Northern Ireland (https://daera-ni.gov.uk) PhD studentship awarded to RA. AK, JH and PMS receive a salary from Boehringer Ingelheim Animal Health; they assisted with academic input and manuscript editing. Otherwise, funders had no role in study design, data collection and analysis, decision to publish, or preparation of the manuscript.

Competing interests: The authors have declared that no competing interests exist.

neurotransmitters, receptors and ion channels, exposing the apparent upregulation of diverse inter-cellular signalling systems. While many neurotransmitter pathways promote proliferation in mammalian systems the interaction between neoblast-like stem cells and neuronal signalling in parasitic flatworms remains elusive. Here, the transcriptomic response of *fhplk1*-RNAi juveniles supports a link between neoblast-like stem cell driven growth/development and neuronal signalling.

Author summary

The liver fluke is a parasitic flatworm which causes disease in livestock and humans around the world. While establishing the infection, immature liver fluke migrate through the host liver causing significant damage. Unfortunately, only one drug is currently recommended for treatment of these immature worms, though resistance to this drug is now widespread and exposes the pressing need to develop novel drugs. As worms migrate through the liver, they undergo growth and development which is facilitated by proliferating stem cells. These neoblast-like cells are akin to stem cells seen in other organisms, and as such are responsible for new tissue growth. Many stem cells express kinases, a large family of enzymes that control many cellular processes. In this study we identified all the potential kinases in the liver fluke, including those that may function in neoblast-like stem cells. One of these kinases, polo-like kinase 1 (PLK1), has been linked to cancer development in humans. We used reverse genetics to silence this gene, allowing us to understand its function. Silencing PLK1 reduced worm growth and stopped neoblast-like cell proliferation, confirming that it has an important role in growth and cell division. Also, we showed that a PLK1 inhibitor, developed for cancer treatments, reduced growth and neoblast-like cell activity, illustrating the potential for targeting liver fluke kinases associated with neoblast-like cells with drugs, providing new routes to drug development. We then carried out RNA sequencing of worms after PLK1 was silenced to show the effects of neoblast-like cell loss on the expression of other genes. We found a decrease in the expression of genes that regulate cell division, but an increase in the expression of genes related to inter-cell signalling, including neuronal genes. This supports evidence for interactions between the nervous system and neoblast-like cells which could be exploited in future drug discovery.

Introduction

Infections with the trematode parasite, *Fasciola hepatica*, can lead to fasciolosis, which is estimated to cause > $3 billion in losses to global livestock yield every year [1]. It also poses a significant threat to human health as a neglected tropical disease [2]. Reports of frontline flukicide (triclabendazole, TCBZ) treatment failure in sheep, cattle and human infections [3], encourage the search for new flukicides, an activity

underpinned by novel drug target discovery and validation [4]. This is necessary as TCBZ is uniquely effective in combatting the migrating, highly pathogenic, juvenile parasites which cause the acute stage of the disease. Furthermore, despite intensive research we do not fully understand the mechanisms of TCBZ action or resistance [3,5,6].

Identification of novel targets that disrupt juvenile *F. hepatica* growth/development could underwrite future control programs. Growth in the related free-living flatworms is driven by neoblasts, somatic stem cells that endow species like *Schmidtea mediterranea* with remarkable regenerative capabilities [7]. These neoblasts are sensitive to irradiation [8], and intriguingly, early attempts to develop *F. hepatica* vaccines with irradiated metacercariae restricted development in a mammalian host [9,10]. If this stunted growth in irradiated *F. hepatica* metacercariae was due to disruption of a neoblast-like cell population, it encourages exploration of neoblast-like cells as targets for future flukicides. Over the last decade a range of studies have identified how proliferating stem cells in several parasitic flatworms, including *Schistosoma mansoni*, *Echinococcus multilocularis* and *Hymenolepis diminuta*, facilitate parasite development and tissue renewal/repair, potentially enabling long-term parasitism within hostile host environments [11–19]. Development of an *in vitro* culture platform for juvenile *F. hepatica* enables juveniles to grow/develop towards an adult-like phenotype and showed that *F. hepatica* growth/development was supported by proliferation of neoblast-like stem cells [20]. Furthermore, a recent study demonstrated that irradiation ablates the neoblast-like cell population of *F. hepatica*, resulting in downregulation of stem cell associated transcripts [21].

Numerous protein kinases (PKs) are associated with proliferating cells. PKs are a diverse group of phospho-transferase enzymes that facilitate transfer of the γ-phosphate on an ATP to a substrate's hydroxyl-group [22]. The human kinome comprises more than 500 PKs [23] that play crucial roles in nearly every aspect of cell biology, with studies suggesting that up to 90% of expressed proteins may be phosphorylated [24]. Functional PKs are typically classed into two groups, the eukaryotic protein kinases (ePKs) and the atypical protein kinases (aPKs) [23]. A staggering 85% of PKs have been linked to cancer or other diseases/developmental disorders [25]. It's unsurprising therefore that there has been intense development of kinase inhibitors over the last 20 years [26], with over 400 currently in clinical trials (https://www.icoa.fr/pkidb/). The critical role of PKs in many cellular processes, and the abundance of kinase inhibitors make their interrogation as putative anthelmintic targets attractive. Indeed, a protein kinase C-β inhibitor (ruboxistaurin) was shown to kill adult *F. hepatica in vitro* [27]. Kinomes have been assembled for several parasitic flatworms, *S. mansoni*, *Schistosoma haematobium* and *Taenia solium* [28–31], illustrating that all nine major PK families are present, and that the kinome represents a similar proportion of the proteome (1.8-1.9%) to that seen in other eukaryotes [23].

The active role of many PKs in the cell cycle/cell division means that mutations or dysregulation can result in cancerous growths [32]. One set of PKs closely associated with the cell cycle are the polo-like kinases (PLKs), named after a mutant form of the *polo* gene which prevented formation of functional spindle poles during cell division in *Drosophila melanogaster* [33,34]. Additional PLKs have been identified throughout the eukaryotes, from yeasts to humans [35–37], where they are implicated in driving cell-cycle progression [38]. PLKs are serine/threonine kinases with a highly conserved domain architecture, comprising an N-terminal kinase domain and a unique, C-terminal polo-box domain that determines subcellular localisation, and is involved in autoinhibitory regulation of the kinase domain [38]. Some organisms only encode a single PLK (e.g., yeast sp.), whereas others possess up to five PLKs, as in humans [38].

Human PLKs1-3 possess a typical PLK conformation, while PLK4 is more divergent and PLK5 lacks an active kinase domain [38]. Polo-like kinase 1 (PLK1) is most akin to *D. melanogaster polo*, with roles in regulating cell cycle progression from the G2/M transition through to cytokinesis. PLK1 promotes mitosis onset through phosphorylation of substrates that allow downstream activation of the cyclin-dependent kinase 1 (CDK1) – cyclin B complex, driving cell entry into M-phase [29,30]. Other roles for PLK1 include promoting disassembly of the interphase centrosome, formation of mitotic spindle, bipolar attachment of microtubules to sister chromatids, anaphase progression and formation of the contractile ring apparatus for cytokinesis [38,39]. PLK1 has also regularly been observed to be overexpressed in cancer tissues, resulting in its appeal as a putative target for cancer therapies [39].

PLK1 has been linked to cell division in *S. mansoni* and *E. multilocularis* [40–43]. PLK inhibition in adult schistosomes reduced gamete production as well as the viability of adults and schistosomula *in vitro* [40,42]. Inhibiting PLK activity in *E. multilocularis* prevented cell proliferation in mature metacestodes and rendered germinative cells unable to form metacestode vesicles *in vitro* [43]. These investigations suggest that targeting PLK activity could represent a broad-acting anti-parasitic flatworm strategy. A gene displaying typical PLK1 domain architecture has been reported in *F. hepatica* (FhPLK1, [44]) and treatment of *ex vivo* immature and adult *F. hepatica* with the PLK1 inhibitor BI 2536 reduced motility and limited adult egg production [45]. Furthermore, recent transcriptomic studies have linked the *F. hepatica plk1* gene, *fhplk1*, with the neoblast-like proliferative cells of *F. hepatica* as it is upregulated in faster-growing worms [46], and downregulated in worms with ablated neoblast-like cells [21].

Here, we have interrogated available *F. hepatica* genomic datasets to generate a *F. hepatica* kinome, identifying 271 putative PKs. Furthermore, we demonstrate that RNA interference (RNAi) of *fhplk1* undermines the neoblast-like cell driven growth of *in vitro*-cultured juveniles. Transcriptomics of *fhplk1*-RNAi worms highlighted downregulation of many cell cycle effectors, alongside upregulation of inter-cell signalling pathways. Additionally, we show that treating juvenile *F. hepatica* with the PLK1 inhibitor BI 2536 *in vitro* phenocopies the effects of *fhplk1*-RNAi by disrupting neoblast-like cell driven growth. Together, these data support the view that FhPLK1 has a conserved role as a cell cycle regulator in *F. hepatica*, enhancing its drug target candidature as a means of disrupting *F. hepatica* growth/development. Furthermore, our transcriptomic datasets facilitate identification of additional drug target candidates and promote our understanding of interplay between *F. hepatica* neoblast-like cells and other tissues.

Results and discussion

The *F. hepatica* kinome

Our bioinformatic screen (S1A Fig) of available *F. hepatica* genomes has enabled us to generate a putative *F. hepatica* kinome. In total, 271 PKs were identified (S1 Table and S1 File) with 254 ePKs and 17 aPKs. This constitutes ~1.6% of the predicted *F. hepatica* proteome, a little smaller than the 1.8-1.9% seen in *H. sapiens*, *S. mansoni*, *S. haematobium* and *T. solium* [23,28–30]. This could be due to the large size of the *F. hepatica* genome, relative to other pathogens [47], or the incomplete nature of the genome assembly, as the total number of PKs identified is comparable to that of *S. haematobium* (269, [30]) and *S. mansoni* (253; updated genome assemblies have removed putative PKs since Grevelding et al. [28]). All putative *F. hepatica* kinase genes were BLASTed (e-value threshold = 0.01) against the *S. mansoni* genome with the top hit recorded. These hits were compared against the *S. mansoni* kinome, revealing that 208/253 predicted *S. mansoni* kinase genes had a matching hit in our *F. hepatica* kinome. Members of all nine ePK families were represented, with calcium/calmodulin-dependent protein kinase (CAMK) and CMGC families found to be the largest (Fig 1A), representing around 30% of all ePKs. These proportions are similar to those of other parasitic helminths, such as *T. solium, Schistosoma* spp., *B. malayi* and *H. contortus* (S1B Fig; [28–31,62,63]). This contrasts with free-living species (*C. elegans*, *D. melanogaster* and humans), where tyrosine kinases (TK) are the largest family (S1B Fig; [23,48,49]), suggesting a reduced role of TKs in parasitism.

The largest *F. hepatica* ePK family (CAMK) contains both substrate restricted and multifunctional kinases with a range of homeostatic roles [50]. Due to their critical roles in Ca^{2+} signalling pathways, they have been proposed as potential anthelmintic targets. Schistosome CAMKII increases its expression/activity following treatment with the paralysis-inducing drug praziquantel, with RNAi reducing motility/viability [51,52], suggesting that CAMKII plays a role in worm motor function/motility. The CMGC family is the second largest ePK family in *F. hepatica.* This highly conserved family consists of members that play critical roles in cell cycle control, such as the cyclin-dependent kinases (CDKs), mitogen-activated protein kinases (MAP kinases) and CDK-like kinases (CDKLs). This high degree of conservation is unsurprising given the crucial role these kinases play in fundamental cell biology, especially in proliferating cells. This may provide opportunities for the development of flukicides that disrupt growth via CDK and MAP kinase inhibition. Indeed, inhibitors targeting

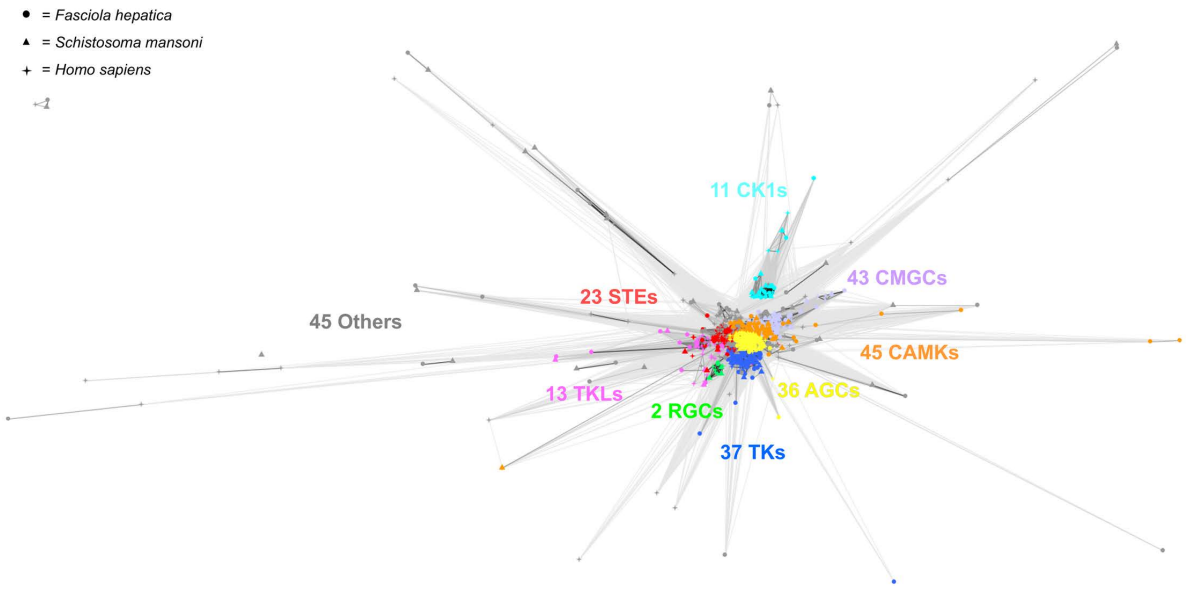


Fig 1. *Fasciola hepatica* exhibit conservation of all major kinase families. CLANs analysis (1M iterations) of *F. hepatica* (circles), *Schistosoma mansoni* (triangles) and *Homo sapiens* (stars) eukaryotic protein kinases shows presence of all nine major families in *F. hepatica* with conservation among CMGC kinases, mitogen-activated protein kinases (STEs), receptor guanylate cyclases (RGCs), casein kinase I (CKs) and calcium/calmodulin kinases (CAMKs), but divergence among tyrosine kinase-like kinases (TKLs).

https://doi.org/10.1371/journal.ppat.1013406.g001

these kinases have already been developed for cancer treatment [53], and repurposing/redeveloping them to target the neoblast-like cells of *F. hepatica* and other parasitic flatworms could lead to their use as novel anthelmintics.

We examined the structural relatedness of *F. hepatica* ePKs alongside *S. mansoni* and *H. sapiens* ePKs using CLANs software, finding the 'Other' grouping to be the most divergent (Fig 1). This was not surprising given the diversity of this group which includes the polo-like kinases, NimA-related kinases and aurora kinases among others. In contrast to this, the AGC, CMGC, receptor guanylate cyclases (RGCs, a family with a catalytically inactive kinase domain similar in structure to tyrosine kinases) and TK families are the most closely clustered, a reflection of their conserved roles across multiple species. The CAMK and casein kinase I (CK1) families clustered closely with only a few divergent members. However, clustering was more diffuse for the tyrosine-like kinases (TKLs) (Fig 1), with *F. hepatica* and *S. mansoni* bone-morphogenic protein receptors (FhHiC23_g1262 and Smp_124450) notable outliers. These bone morphogenic protein receptors may be druggable targets, especially with only a 24–35% amino acid sequence identity when compared to human bone morphogenic protein receptors. Recent publications in *F. hepatica* have demonstrated the potential of targeting kinases (protein kinase C β and p21-activated kinase 4) to disrupt motility/viability [27,54].

We also identified 17 putative *F. hepatica* aPKs (S1 Table), functional PKs with a typical catalytic kinase fold that lack sequence similarity to ePKs [55]. As in other organisms, there are considerably fewer aPKs than ePKs, though the number identified here is comparable to that found in *C. elegans* [56]. Several conserved *F. hepatica* aPKs (S1C Fig) play vital roles in cell proliferation, potentially linking them to their neoblast-like stem cells, such as mammalian target of rapamycin (mTOR), ataxia–telangiectasia mutated kinase (ATM), ataxia–telangiectasia and Rad3 related kinase (ATR) and the phosphoinositide 3-kinases [57–59], again highlighting numerous pathways that could be exploited for juvenile fluke control.

FhPLK expression linked to developing juveniles

We used published life-stage transcriptomic data [47] to examine expression profiles of putative PKs. Of the 266 kinases for which we have life stage transcriptomic data, 116 show the highest relative expression in NEJs or immature worms

(migrating three-week-juveniles) (S1D Fig). Seven of these genes with enriched expression are *cdk*s, crucial cell cycle regulators [60]. Among them is a putative *cdk1* gene (FhHiC23_g16347), a critical component of M-CDK that drives the cell into mitosis, which has also been implicated in regulating the pluripotency of embryonic stem cells [61], and can drive the cell cycle in early embryonic cells lacking all other CDKs [62]. Additionally, four putative *F. hepatica* fibroblast growth-factor receptors (*fgfrs*) and two *plks* are most highly expressed in these developing life stages. We also utilised a published transcriptomic dataset that compared *in vitro F. hepatica* juveniles with faster-growing *in vivo* juveniles [46] and found 81% of kinases were more highly expressed in the faster-growing *in vivo* juveniles (S1D Fig), again supporting the hypothesis that kinases play an integral role in growth/development.

Development-associated kinases were further interrogated using the *F. hepatica in vitro*/*in* vivo transcriptomic datasets [46] alongside a dataset which identified genes associated with *F. hepatica* neoblast-like cells [21]. Six kinases were downregulated following neoblast-like stem cell ablation, and 21 kinases were upregulated in faster-growing worms (S2 Table). Notably, two genes were prominent in both of these datasets, a *fgfr* (FhHiC23_g5821) and *plk1* (FhHiC23_g6132). FGFRs are tyrosine-kinase receptors linked to proliferation [63] with drug inhibition, RNAi or CRISPR-interference in *S. mansoni* and *E. multilocularis* reducing neoblast-like cell proliferation [11,12,64,65]. Three FGFR inhibitors have been approved by the FDA for treatment of cancers and idiopathic pulmonary fibrosis [66], highlighting the druggability of these kinases.

PLK1 is a core cell cycle effector, regulating centrosome assembly, mitotic entry, the spindle, cytokinesis and more besides [39]. PLK1 has been linked to cell differentiation and survival in other parasitic flatworms [40–43], while in *F. hepatica* its downregulation following irradiation and upregulation in faster growing worms (S2 Table) support its link with neoblast-like stem cells. Our HMM screen and additional BLAST searches identified two further putative *F. hepatica* PLKs (FhPLK2 [FhHiC23_g13468] and FhPLK4 [FhHiC23_g6087]; Fig 2A). These genes are distinct from each other, sharing only 25–27% identity at the amino acid level with only FhPLK1 predicted (full sequence confirmed using transcriptomic reads) to possess all signature PLK1 domains (Fig 2C), including the ATP-binding motif [67], catalytic motifs, Mg^{2+} chelating motif [68], phosphorylation site [69] and phosphopeptide binding sites [70,71]. Published life stage transcriptomic data [47] show that *fhplk1* expression peaks in eggs (Fig 2B), potentially indicating significant proliferative cell activity as the embryo develops into the unhatched miracidia, like that seen in *S. mansoni* [72]. Following eggs, relative expression was highest in immature worms and adults, life stages with significant neoblast-like stem cell and germ cell activities respectively [46,73,74]. Moreover, transcriptomic data from Robb et al. (Fig 2B, [46]) show greater *fhplk1* and *fhplk4* expression in faster-growing *in vivo* worms, correlating with observed increased cell proliferation. Houhou et al. [44] also found higher *fhplk1* expression in immature worms and adults compared to NEJs (24 h post-excystment) via PCR, though they also observed ~6-fold increase in expression in adults compared to immature worms. The difference seen here between transcriptomic and qPCR methodologies could be due to low replicate numbers in the published transcriptomic datasets [47]. As *plk1* has previously been localised to *S. mansoni* reproductive structures [40], the increased expression in adult *F. hepatica* is likely associated with germ cell activity in this life stage. Together, these transcriptomic data indicate that *fhplk1* is associated with cell proliferation in *F. hepatica*.

RNAi-mediated gene silencing of *fhplk1* disrupts juvenile growth

To test if *fhplk1* is integral to maintenance of the *F. hepatica* neoblast-like cell population we employed RNAi to probe its function *in vitro*. Parasites were treated with *fhplk1*-specific dsRNA and monitored for signs of abnormal growth. Transcript knockdown of *fhplk1* was measured after four weeks and found to be reduced by ~90% relative to control treatment (Fig 3A; mean transcript expression ±SEM: control dsRNA = 127.67 ± 9.49%, *fhplk1* dsRNA = 9.33 ± 2.73%). We also found that transcript expression of another proliferative cell marker (histone 2b (*fhh2b*)) was reduced by 81.7 ± 9%. Though not significantly different, it suggested that *fhh2b* expressing cells were depleted in *fhplk1*-RNAi worms; expression of a muscle cell marker (myosin light-chain (*fhmlc*)) was reduced by 21.3 ± 30% relative to untreated worms, although again

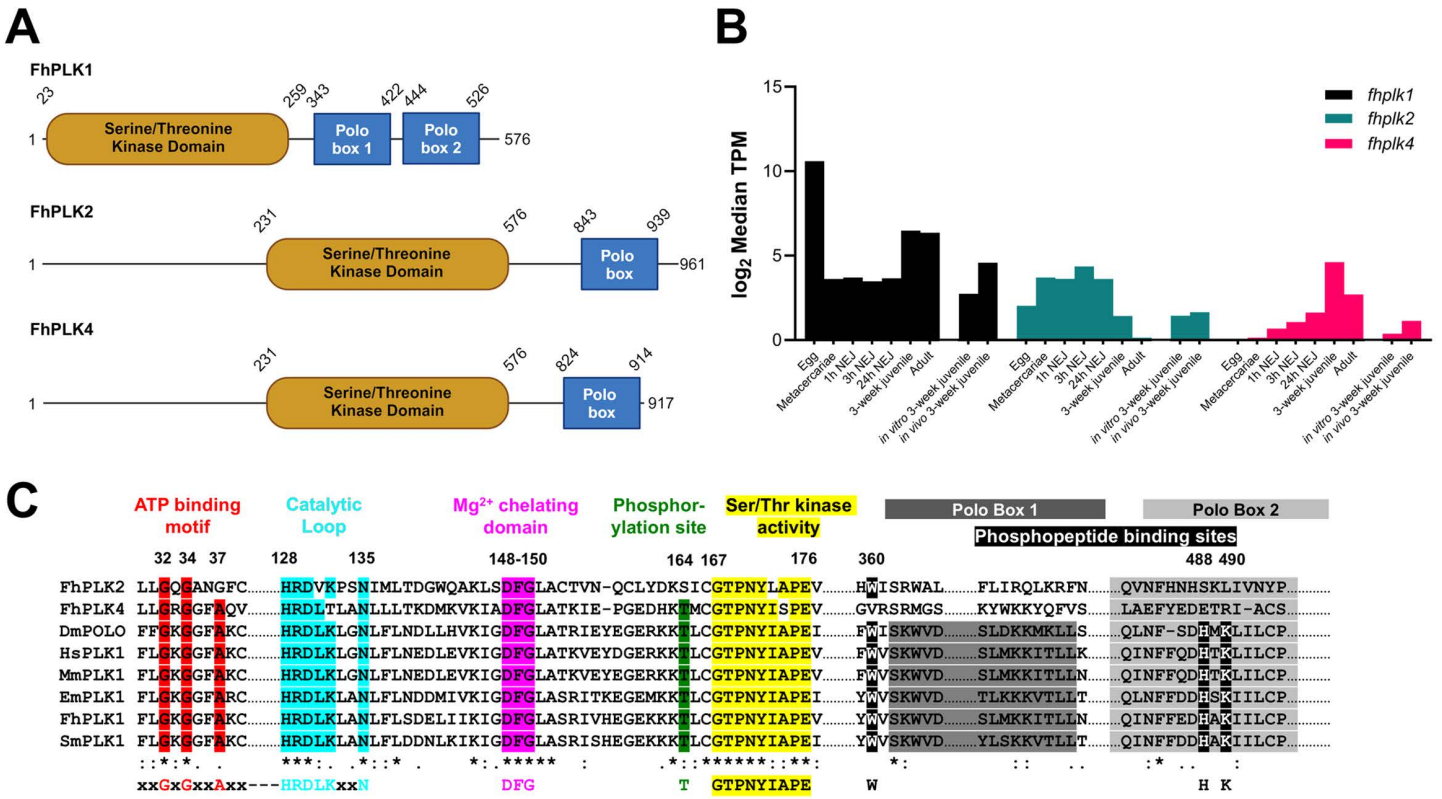


Fig 2. ***Fasciola hepatica*** **polo-like kinase 1 (PLK1) possesses all functional kinase domains. (A)** Schematic of *F. hepatica* PLKs, with domains as predicted by Interpro, illustrating N-terminal serine/threonine kinase domains and C-terminal polo-boxes. **(B)** Expression of *fhplk* genes from published datasets; Log_2-transformed median transcripts per mapped million reads (TPMs) of *F. hepatica plk* genes across various life stages (egg, metacercariae, 1h NEJ, 3h NEJ, 24h NEJ, 3-week juvenile, adult; n = 1–3 for each lifestage; [47]); Log_2-transformed median transcripts per mapped million reads (TPMs) of *F. hepatica plk* genes in *in vitro and in vivo* 3-week juveniles (n = 3 for each treatment; [46]). **(C)** Conservation of functional motifs in FhPLK1 but not FhPLK2/4 when compared to PLK1 sequences from *Echinococcus multilocularis*, *Schistosoma mansoni*, *Drosophila melanogaster*, *Homo sapiens* and *Mus musculus*; * = conserved residue,: = highly conserved amino acid properties,. = weakly conserved amino acid properties (our transcriptomic reads were used to confirm sequence).

https://doi.org/10.1371/journal.ppat.1013406.g002

this was not significant (Fig 3A). H2B is highly expressed throughout the S-phase of the cell cycle when it participates in chromatin organisation [75], with RNAi-mediated silencing in free-living and parasitic flatworms impairing cell proliferation [12,16,21,76], therefore demonstrating how *plk1*-RNAi in *F. hepatica* has led to the depletion of a proliferative cell-associated transcript. Here, we observed that *fhplk1*-RNAi affected fluke development *in vitro*, with *fhplk1*-RNAi juveniles significantly smaller than control worms three weeks after the first RNAi trigger (Fig 3B; mean juvenile area ±SEM at three-weeks: untreated = 97350 ± 2559 μm², control-dsRNA = 94214 ± 4266 μm², *fhplk1* dsRNA = 73964 ± 2559 μm²). This phenotype was further exaggerated after a fourth week (Fig 3B; mean juvenile area ±SEM at four-weeks: untreated = 118368 ± 4732 μm², control-dsRNA = 117781 ± 5130 μm², *fhplk1* dsRNA = 75942 ± 2495 μm²). We also found that *fhplk1* knockdown impaired cell proliferation in four-week-old juveniles, thereby disrupting the neoblast-like stem cell population (Fig 3C and 3D; mean # 5-ethynyl-2-deoxyuridine $(EdU)^+$ nuclei ±SEM: control-dsRNA = 477.5 ± 47; *fhplk1*-dsRNA = 9.8 ± 5.4). RNAi of *plk1* in mammalian cancer cell lines *in vitro* also reduced proliferation [77], and reduced tumour size *in vivo* in mice with non-small cell lung carcinoma [78], supporting a conserved role for *plk1* in proliferative cells. Interestingly, following four weeks of *plk1* silencing, juveniles cultured for a week in the absence of a RNAi-trigger showed no signs of recovery and did not resume proliferation (S2 Fig); this observation is consistent with the hypothesis

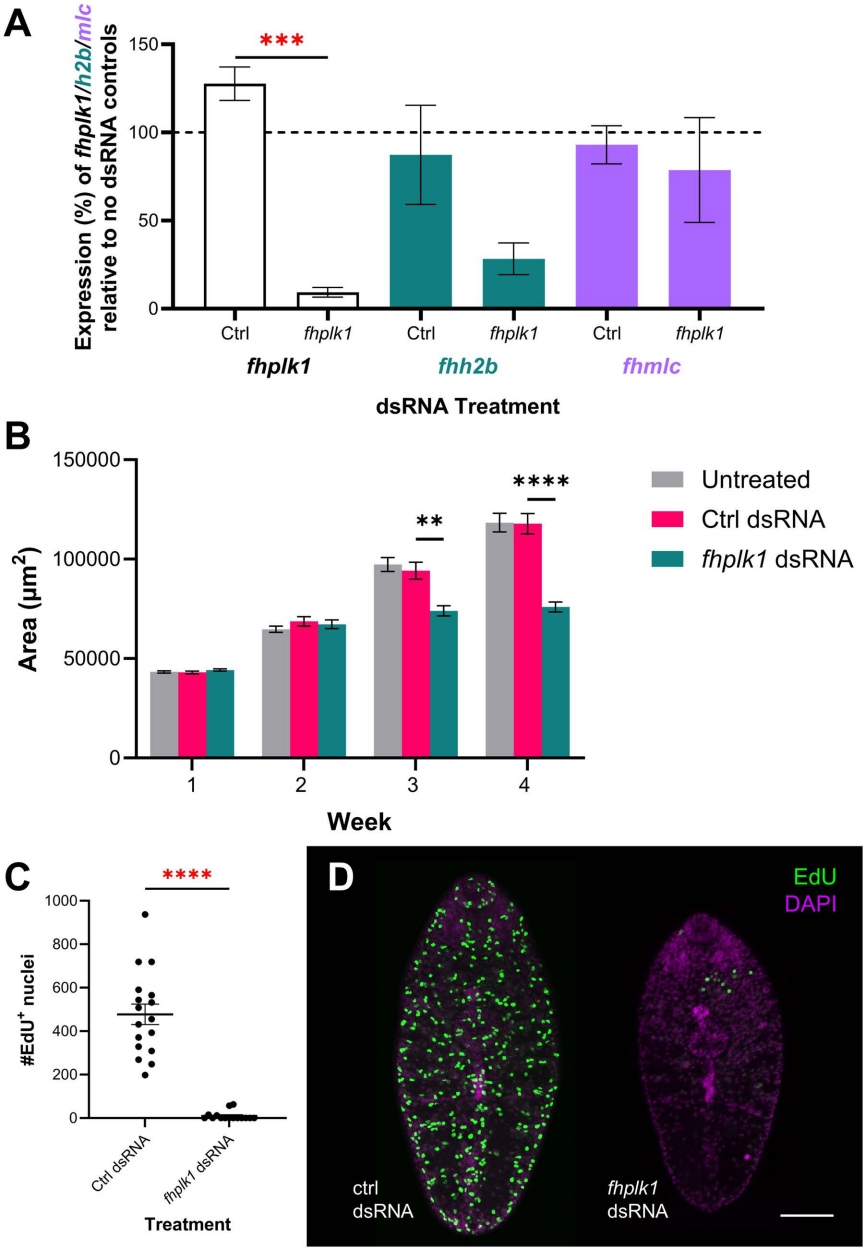


Fig 3. Knockdown of *fhplk1* disrupts growth and cell proliferation in juvenile *Fasciola hepatica in vitro*. **(A)** Mean expression ±SEM of *fhplk1* (white), *fhh2b* (green) and *fhmlc* (purple) in dsRNA-treated juvenile *F. hepatica* relative to no dsRNA-treated juveniles following four weeks of repeated exposures to *fhplk1* dsRNA *in vitro* shows significant knockdown of *fhplk1* and reduction in expression of neoblast-like cell associated gene *fhh2b* relative to control dsRNA treated worms (n = 3 for each treatment, unpaired t tests). **(B)** Mean area ±SEM of juvenile *F. hepatica* significantly diminished over three/four weeks of *fhplk1* dsRNA exposures (n ≥ 37 for each treatment; Kruskal-Wallis and Dunn's posthoc tests). **(C)** Mean # EdU⁺ nuclei ±SEM significantly decreased after four weeks of *fhplk1* dsRNA treatments in juvenile *F. hepatica* (n ≥ 15 for each treatment; Mann-Whitney U test). **(D)** Confocal images of EdU staining (green) in four-week-old *F. hepatica* treated with *fhplk1* dsRNA *in vitro* shows reduction in # EdU⁺ nuclei compared to control dsRNA treated worms; scale bar = 100 µm, DAPI counterstain (magenta). **, p < 0.01; ***, p < 0.001; ****, p < 0.0001.

https://doi.org/10.1371/journal.ppat.1013406.g003

that prolonged *fhplk1*-RNAi results in the ablation of *F. hepatica* neoblast-like stem cells. It is possible that if culture was continued for longer in the absence of a RNAi-trigger, proliferative cells could recover if the systemic effects of RNAi do not persist. Together, these data support a conserved function for PLK1 in *F. hepatica* that ensures cell-cycle progression. As PLK1s are functionally conserved in *S. mansoni* and *E. multilocularis* [40,43], targeting PLK1 activity could be an effective pan-phylum control strategy.

RNAi of *fhplk1* downregulates cell cycle effectors and ribosome biogenesis

We previously used irradiation to identify transcripts associated with *F. hepatica* neoblast-like cells [21]. However, while irradiation is effective at ablating proliferating cells, the potential for damage to differentiated cells limits its utility. Transcriptomic analysis following *fhplk1* silencing would help inform the role of *fhplk1* role in juvenile fluke and support identification of other genes associated with growth/development. Therefore, we carried out target-specific RNAi for three weeks before RNA extraction and transcriptome sequencing (Fig 4A), confirming that *fhplk1*-RNAi reduces growth and ablates neoblast-like stem cells (S3A and S3B Fig). RNA-Seq was then used to identify differentially expressed genes (DESeq2, padj < 0.001; S4 Table), with 946 downregulated genes and 1244 upregulated genes (Fig 4B). TOPGO analysis showed that genes associated with protein translation, ribosome assembly and DNA replication were overrepresented among downregulated genes (Fig 4C). Many of these GO terms are also overrepresented among genes associated with the germinative cells found in *E. multilocularis* [79]. The downregulation of genes associated with protein synthesis ('translation' and 'protein folding'; Fig 4C) was interesting as studies in mouse cells showed that protein synthesis rates in early differentiated mouse cells are two-fold of that in embryonic stem cells [80], a result also observed in other mammalian cell cultures (reviewed in [81]). As *fhplk1*-RNAi depletes neoblast-like cells (i.e., stem cells) the proportion of differentiated cells might be expected to increase relative to control worms, although the production of more undifferentiated cells in the control groups could explain the higher levels of protein synthesis. Further, other GO terms ('ribosomal small subunit assembly', 'structural component of ribosome'; Figs 4C and S3C) suggested that the downregulation of translation may be related to reductions in ribosomal activity. KEGG pathway analysis showed the downregulation of ribosomal subunits/biogenesis following *fhplk1*-RNAi (S3D Fig) which matches observations in other platforms where stem cells have lower translation rates than differentiated cells, except in the case of ribosome biogenesis, which is upregulated in proliferating cells [82]. The downregulation of ribosome biogenesis-associated genes was also observed 14 days after irradiation in *S. mansoni* [13], demonstrating that this occurs in related species. It is also possible that the differential expression of ribosome-associated genes/pathways is indicative of general stress, as downregulation of these genes/pathways has previously been noted in nematodes following drug treatment (with non-stem cell targeting drugs) and local environment change [83,84].

Transcripts associated with DNA/RNA interactions and the cell cycle were also downregulated following *fhplk1* knockdown (e.g., DNA-replication initiation; Figs 4C, 4D and S3). Indeed, 4/5 KEGG pathways downregulated following irradiation of *F. hepatica* juveniles [21] were downregulated following *fhplk1* RNAi (S3D Fig). Numerous core cell cycle genes were downregulated (Fig 4D and S3 Table), including *atm* and *atr* kinases, cell division control proteins, *cyclinB*, members of the mini-chromosone complex (*mcm2–7*) and origin recognition complex subunits (*orc2 & 3*). Additional core cell cycle regulators not annotated by eggNOG, but identified through BLAST searches, were also downregulated, such as a p53 homologue (FhHiC23_g6525). p53 is a tumour suppressor which can arrest the cell cycle and cause apoptosis when activated [85]. Mutations in p53 are linked to cancerous growths, with compounds developed to reverse these adverse mutation effects currently in clinical trials [86]. Furthermore, a *S. mansoni* p53 homologue has been linked to their neoblast-like cells [18]. While many of the cell cycle effectors discussed likely have conserved structure/function in both parasites and their hosts, inhibitors that indirectly target them [87] may be worth exploring for their anthelmintic potential. One surprising observation in the cell cycle schematic was 'upregulation' of *fhplk1* following *fhplk1* RNAi (DESeq2, *fhplk1* $\log_2$Fold Change = ↑ 3.73). Our earlier trials had confirmed *fhplk1* knockdown following dsRNA treatment via qPCR (Fig 3A), so this upregulation was unexpected.

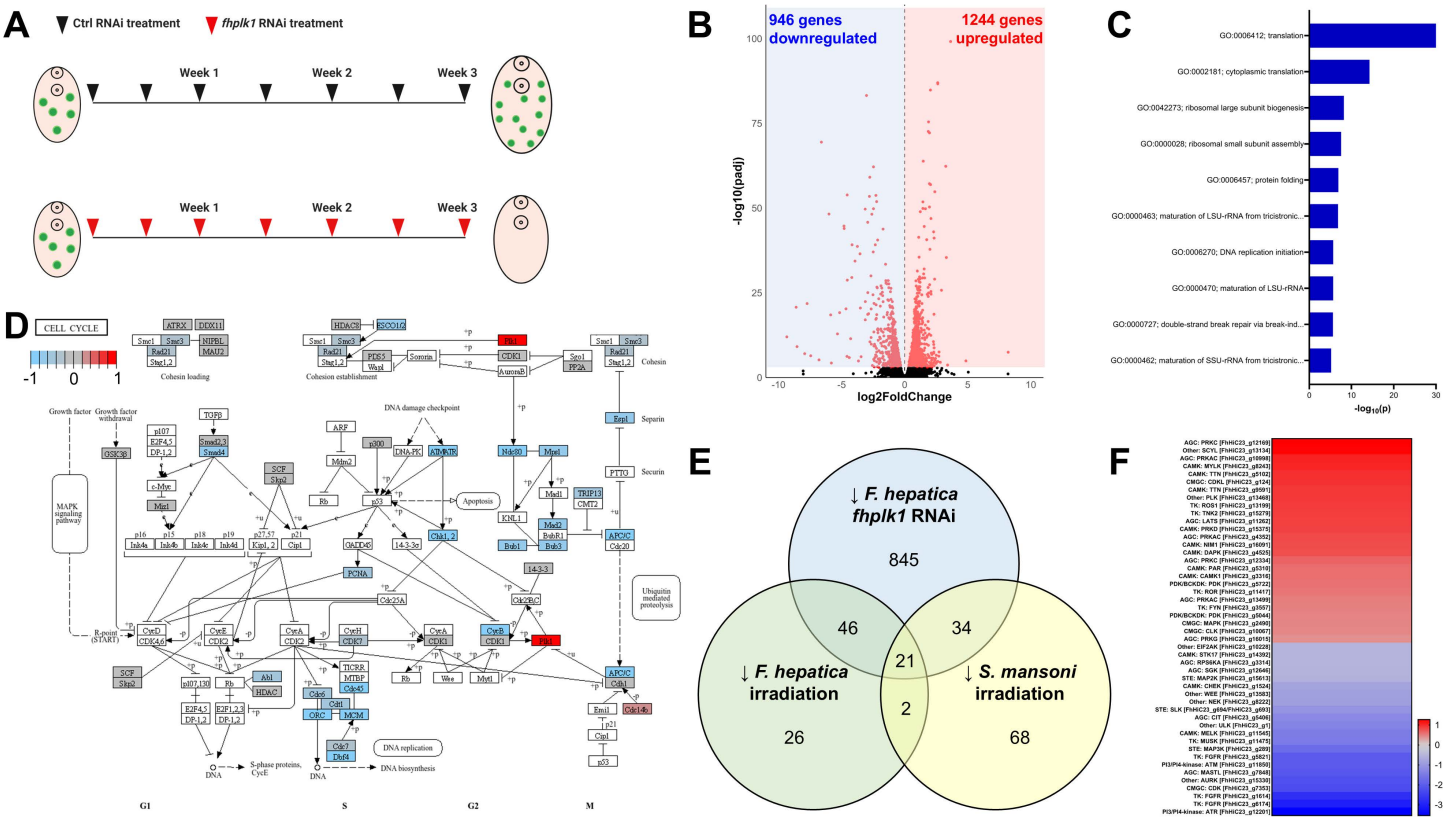


Fig 4. *fhplk1* knockdown downregulates cell cycle and translation-associated transcripts in juvenile *Fasciola hepatica in vitro*. (A) Experimental timeline showing dsRNA treatments (24 h dsRNA exposure each time) carried out on juvenile *F. hepatica* across three weeks to generate transcriptomes with final treatment from day 21–22. (B) Volcano plot showing differentially expressed genes (red dots; DESeq2, padj < 0.001) after *fhplk1* RNAi in juvenile *F. hepatica* where blue shading indicates downregulated genes and red shading indicates upregulated genes. (C) Top 10 overrepresented biological process GO terms among downregulated genes following *fhplk1* RNAi shows genes involved in translation and nucleotide interactions. (D) Many components of KEGG cell cycle pathway downregulated following *fhplk1* RNAi (red = upregulated; grey = no change; blue = downregulated; white = unassigned KEGG ID). (E) Venn diagram showing overlap between genes downregulated following *fhplk1* RNAi in juvenile *F. hepatica* (blue), irradiation in juvenile *F. hepatica* (green) or irradiation in adult *S. mansoni* (yellow). (F) Log_2foldchange of differentially expressed kinases following *fhplk1* RNAi shows downregulation of proliferation-associated kinases such as MAPKs and FGFRs (colours correspond to log_2foldchange; red = upregulated; blue = downregulated). Experimental timeline schematic created in BioRender.

https://doi.org/10.1371/journal.ppat.1013406.g004

However, examination of the read files via the Integrative Genomics Viewer (https://igv.org/) revealed that *fhplk1* dsRNA was likely sequenced as reads were observed only in the 192 bp dsRNA amplicon region of *fhplk1* dsRNA samples (S3E and S3F Fig). Control dsRNA samples on the other hand had reads across the length of the gene, with exons clearly visible (S3E Fig). The data indicate that this sequencing anomaly is related to our RNAi methodology as we ensure knockdown by repeatedly soaking worms in 100 ng/μL dsRNA) [88], including the 24 h period immediately preceding worm extraction.

We aimed to identify pan-trematode transcripts clearly linked to parasitic flatworm neoblast-like cells by cross-referencing the transcriptomic data generated here against the transcriptomes of irradiated *F. hepatica* and *S. mansoni* (orthologues were identified based on the top hit in BLAST searches against the *S. mansoni* genome and can be found in S3 Table) [12,21]. We found 21 genes downregulated in all three transcriptomic datasets following neoblast-like cell ablation (Fig 4E; note that the relatively small number of downregulated genes found in both irradiated datasets is likely due to the different life stages investigated as discussed in [21]). Many of the genes downregulated in all three datasets are known for their links to proliferation (S4 Table), including the cell cycle regulators *p53*, *cyclinB* and the *mcm* complex

members. A further 34 genes were downregulated following *fhplk1*-RNAi in *F. hepatica* and irradiation in *S. mansoni*, including *hepatic leukaemia factor*, *mastL* (*greatwall kinase*) and *wdhd1* (*WD repeat and HMG-box DNA-binding protein/and-1*) which again have been associated with cell cycle regulation [89], DNA replication [90] and stem cell population maintenance [91] in *Xenopus*/human cells. Finally, 46 genes were downregulated in *F. hepatica* following either *fhplk1*-RNAi or irradiation with eight transcription factors/regulators included among them as well as a *fgfr*, implying conserved roles related to *F. hepatica* neoblast-like cells. While there were these shared downregulated genes between these two *F. hepatica* datasets there were 879 genes only downregulated following *fhplk1*-RNAi (Fig 4E). We hypothesise that this difference is caused by the loss of neoblast-like cells over an extended 3-week period of time (unlike the irradiated dataset in which juveniles were sequenced 48 hours after X-ray exposure), with this having knock-on effects across tissues in the worm.

As several of the genes downregulated in both datasets were kinases we explored the expression of all *F. hepatica* kinases following *fhplk1* RNAi; 48 kinases were differentially expressed (22 downregulated and 26 upregulated; Fig 4F). Among downregulated kinases were three *fgfrs* that were also upregulated in developing life stages (FhHiC23_g6174, FhHiC23_g1614 and FhHiC23_g5821), an aurora kinase and members of the MAPK signalling cascade which regulates cell cycle progression [92]. Again, these kinases are integral to activate proliferation in other species and may be appealing targets for control. AGC kinases and CAMKs were more represented among upregulated kinases, though their functions are more diverse and less clearly linked to proliferation.

One final point to note is that of 46 genes downregulated after irradiation or *fhplk1*-RNAi in *F. hepatica*, ten had no clear BLAST hit in model species, though they all have *S. mansoni* homologues and most have *F. gigantica* homologues. Furthermore, of the 50 most downregulated transcripts (ranked by fold-change) only 8 had clear BLAST hits in model species (e-value <0.001, S3 Table), though most were found to have orthologues in at least one other parasitic flatworm. While we know little of the function of these genes/proteins, their downregulation links them to putative roles in *F. hepatica* growth/development associated with neoblast-like stem cells, especially where also downregulated following irradiation. These unknown genes could eventually become attractive drug targets, given their lack of homology to genes in host species.

Inter-cell signalling upregulated following *fhplk1* RNAi

Over 1200 juvenile fluke genes were upregulated following three weeks of *fhplk1*-RNAi (Fig 4B and S3 Table). TOPGO analysis of these genes showed that GO terms associated with inter-cell signalling systems such as ion transport, cell-adhesion and synapses were overrepresented (Figs 5A and S4A) among the upregulated genes. Furthermore, cellular component GO terms suggested many predicted proteins are associated with the cell membrane and extracellular space/synapse (S4A Fig), supporting evidence for the upregulation of inter-cell signalling. KEGG pathway analysis further reinforced this, highlighting upregulation of multiple neuronal-ligand receptors, including many GPCRs (Fig 5B). Many signalling pathways were also upregulated, such as those linked to the gap junction as well as GABAergic, serotonergic and cholinergic synapses (S4B Fig). Gap junctions are critical to cell-cell connectivities that help coordinate cellular functions in multicellular organisms, though invertebrates lack the associated connexin proteins and instead possess innexins [93]. Interestingly, a recent study in *S. mediterranea* identified two innexins that appear to play roles in stem cell response to injury [94]. While the gap junction itself is unmarked in the KEGG pathway of S4C Fig as the pathway is based on that of humans, we found five predicted innexins to be significantly upregulated following *fhplk1*-RNAi (FhHiC23_g648, FhHiC23_g6222, FhHiC23_g9940, FhHiC23_g15433 and FhHiC23_g15004; S3 Table). Innexins have been localised in various planarian tissues, including the nervous system [95], and their inhibition can lead to developmental abnormalities through polarity disruption during regeneration [95,96], or ablation of neoblast-cell populations [97], suggesting key roles in developmental regulation.

Within the upregulated classical transmitter pathways there was upregulation of ligand synthesis enyzmes, receptors and downstream signalling molecules such as G proteins (serotonergic example shown in S4D Fig). Indeed, of the known

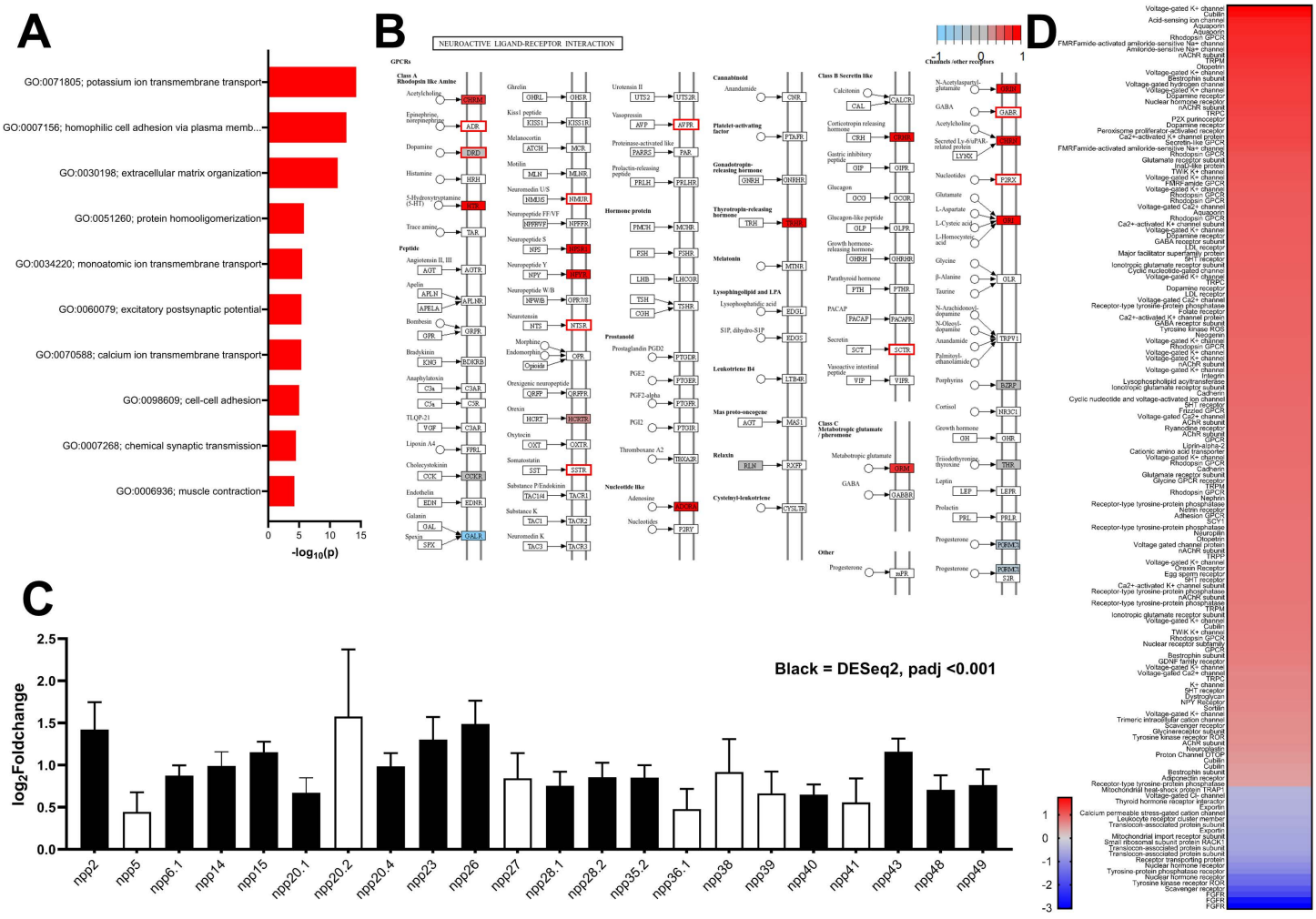


Fig 5. RNAi of *fhplk1* in *Fasciola hepatica* results in upregulation of inter-cell signalling systems. (A) Biological process GO terms (top 10) associated with ion transport and cell signalling are overrepresented among upregulated genes following *fhplk1* RNAi. **(B)** KEGG pathway showing upregulation of several neuroactive-ligand receptors following *fhplk1* RNAi (red = upregulated; grey = no change; blue = downregulated; white = unassigned KEGG ID; red box = unassigned KEGG ID but identified as upregulated from BLAST searches). **(C)** Log_2foldchange ±SEM of putative *F. hepatica* neuropeptides following *fhplk1* RNAi shows all 22 upregulated, with 15 differentially expressed (black bars). **(D)** Log_2foldchange of differentially expressed putative receptors and channel subunits (identified via BLAST searches) following *fhplk1* RNAi shows upregulation of 134/155 (n = 3; colours correspond to log_2 foldchange; red = upregulated; blue = downregulated).

https://doi.org/10.1371/journal.ppat.1013406.g005

F. hepatica classical transmitter pathways [98], only the histamine pathway had no evidence (based on TOPGO, KEGG and BLAST analysis) of upregulation, a poorly understood pathway in parasitic flatworms [99]. Curiously, some upregulated classical transmitter pathways have opposing effects on *F. hepatica* motility (e.g., acetylcholine is believed to be inhibitory [100], while serotonin is excitatory [101]), making their concurrent upregulation interesting and potentially linked to increased tonic regulation. Serotonin has been implicated in proliferation in other species [102–105] and has been shown to directly stimulate growth/proliferation in *S. mansoni* and *E. multilocularis* [106,107]. While the roles of acetylcholine and dopamine in flatworm growth are unknown, they have been linked to proliferation in mammals [108,109]. Furthermore, dopamine deficiency in *C. elegans* and *D. melanogaster* constrains development [110,111] and a dopamine antagonist reduced *S. mansoni* miracidial transformation [104]. *C. elegans* lacking choline acetyltransferase (ChAT) also display slower growth [112].

Additionally, 16/22 putative neuropeptide encoding genes identified in our dataset (S5 Table) were significantly upregulated in *plk1*-RNAi worms (Fig 5C), as were their processing enzymes; *prohormone convertase 2* (*pc2*; FhHiC23_g9059), *carboxypeptidase E* (*cpe*; FhHiC23_g10997), *peptidylglycine alpha-hydroxylating monooxygenase* (*phm*; FhHiC23_g3039) and *peptidyl-alpha-hydroxyglycine alpha-amidating lyase* (*pal*; FhHiC23_g9107), along with several predicted neuropeptide receptors (Fig 5B). Neuropeptides have been shown to drive mammalian cell proliferation [113], as well as germline proliferation and regeneration in planarians [114–117]. Furthermore, two neuropeptides and their GPCRs are required for normal maturation of female reproductive structures in *S. mansoni* [118]. If classical transmitters and neuropeptides have conserved roles in managing growth/proliferation in *F. hepatica,* then the upregulation observed could indicate that *fhplk1*-RNAi juveniles lacking neoblast-like cells are attempting to boost cell proliferation via enhancement of selected inter-cell signalling systems.

Previously, we highlighted that signalling systems were upregulated in slower growing *F. hepatica* with decreased cell proliferation [46]. Here we saw the loss of neoblast-like stem cells, concomitant with nervous system upregulation, indicating potential interplay between proliferating neoblast-like stem cells and neuronal signalling systems. When we compared upregulated genes in our neoblast-like stem cell ablated juveniles with downregulated genes in neoblast-like stem cell-enriched *in vivo* juveniles [46], we identified 244 shared genes, including 12 neuropeptide encoding-genes (S6 Table). Further, TOPGO analysis of these genes showed that neurotransmitter and Wnt signalling were enriched (S4E Fig). Enrichment of the Wnt pathway is notable as Wnts support proliferation and polarity orientation in regenerating planarians [119], with similar roles proposed in parasitic flatworms [120–122]. RNAi of *wnt* genes in regenerating planarians can result in aberrant neurogenesis [123–126] and their silencing was recently shown to inhibit *F. hepatica* neoblast-like cell proliferation and growth/development *in vitro* [127].

To help us understand the scale of signalling upregulation we examined all BLAST results for the terms ‘receptor’ or ‘channel’ to identify putative intercellular signalling-related genes. Of the 155 putative receptors/channels identified through BLAST searches, 134 (86%) were significantly upregulated following *plk1*-RNAi (Fig 5D). Those that were downregulated were mainly kinases or nucleus-associated receptors that could be associated with worm neoblast-like stem cells. S4G Fig shows that 22% of the upregulated receptors/channels were predicted rhodopsin peptide GPCRs with voltage-gated potassium channel subunits constituting another large component. Among these genes were two putative FMRFamide-activated amiloride-sensitive Na+ channel subunits [128] that may be of interest as putative drug targets due to their unusual pharmacology and proposed absence in mammals. These data illustrate the extent of upregulation seen within signalling systems following sustained *fhplk1*-RNAi.

We recognise that the reduced size of *plk1*-dsRNA worms (in comparison to control dsRNA worms) may increase the proportionality of neuronal tissue, thereby increasing the balance of neuronal-associated transcripts. However, tissue proportionality does not appear to be a key factor in the observed upregulation for a variety of reasons. Firstly, while *fhplk1*-RNAi worms were indeed smaller (S3A Fig), the difference in size was modest compared to that seen in the gene-function RNAi trials (Fig 3B). Furthermore, while we found DAPI staining (calculated as a percentage of worm area) decreased following *fhplk1*-RNAi (S4F Fig), the decrease was ~ 20% which may be directly attributable to the absence of neoblast-like stem cells (neoblasts account for around 20–35% of all cells in free-living flatworms [129]). Second, another study observed the downregulation of signalling systems in faster growing, stem cell enriched *F. hepatica* [46], with much greater size differences (~15x) than those observed in our study. Despite this, genes associated with signalling had comparable fold changes in expression in most instances (S7 Table), again suggesting size/tissue proportionality is not a factor in nervous system upregulation. Thirdly, we did not observe consistent upregulation of transcripts associated with other tissue types, such as the tegument (*tsp2*) or the gut (18 cathepsins upregulated and 14 downregulated) which indicates that the nervous system transcript upregulation is unusual. Finally, we found this pattern of increased signalling in adult male *S. mansoni* datasets in which worms were subjected to transcriptomics two weeks after irradiation, or three weeks after the onset of *smfgfrA* or *smh2b* RNAi [13]. TOPGO analysis of these datasets showed again that there was

an increase in transcripts associated with signalling systems, ion transport and cell communication (S8 Table). Given that these worms were adults of comparable size and that the anterior portion, including cerebral ganglia, had been removed (to exclude testes from analysis) the upregulation of signalling systems following neoblast-like stem cell ablation in diverse circumstances supports the validity of these transcriptional changes in neuronal signalling systems and warrants further investigation.

These data challenge the traditional orthodoxy of using short-term motility-based assays to assess the drug target candidature of various helminth signalling pathways. If the signalling systems highlighted in this study do play significant roles in cell proliferation, then potential long-term impacts of drugs on worm growth/development could be missed with restricted phenotype monitoring windows. Glutamate-gated chloride channels and nicotinic acetylcholine receptors are already targets of current anthelmintics, while GPCRs are thought of as highly 'druggable' targets [130]. Repurposing drugs to disrupt neoblast-like stem cell biology could expose novel control strategies.

No correlation between DE miRNAs and predicted DE mRNA targets

We carried out miRNA sequencing on the same RNA samples and used miRDeep2 to map reads to the 150 predicted miRNAs [131]. We found 68 of these miRNAs were expressed in at least two of the six samples, with 13 downregulated and 8 upregulated (S5A Fig; DESeq2, padj <0.001; S9 Table). Target prediction software was then used to identify putative target transcripts of these differentially expressed miRNAs (S9 Table). TOPGO analysis did not identify any enriched GO terms among potential target transcripts. We then plotted GO term frequency of predicted target transcripts against fold change (S5B Fig) but found little, to no overlap with GO terms of differentially expressed mRNAs. Finally, only 36 targets predicted to be downregulated were found to be so, while only 38 of those predicted to be upregulated were so. No clear links between *fhplk1*-RNAi silencing in juvenile *F. hepatica* and endogenous miRNA activity were uncovered.

Pharmacological inhibition of FhPLK1 phenocopies *fhplk1*-RNAi

We next targeted FhPLK1 using the commercially available inhibitor BI 2536. Overexpression of PLK1 in various cancers has led to the development of inhibitors, including BI 2536, a highly selective PLK1 inhibitor which can blunt cell proliferation in various cancer types, both *in vitro* and *in vivo* [132,133]. As BI 2536 is an ATP-competitive inhibitor [132], high levels of sequence similarity across human PLK1–3 kinases compromises its selectivity [132,133]. As discussed previously we identified two additional PLK genes in *F. hepatica*, one similar to human PLK2 (FhPLK2), with the other similar to both human PLK4 (FhPLK4) and SAK (Serum-inducible kinase Akin Kinase) in *S. mansoni* and *E. multilocularis* [43,134]. PLK4 divergence in humans renders it less sensitive to BI 2536 [132], a trait also observed for *S. mansoni* SmSAK [134]. Crystallisation experiments identified Leu_{132} of HsPLK1 as a key residue for facilitating drug-target interaction and selectivity. This leucine was conserved in FhPLK1 (Leu_{104}), but not in FhPLK2 or FhPLK4 (S6A Fig), suggesting that the activity of BI 2536 would be specific to FhPLK1 in *F. hepatica*.

Initial experiments involved exposing NEJs to a broad range of BI 2536 concentrations (0.001 μM – 10 μM) for 18 hours in RPMI, with motility measured as an indicator of viability as motility of *F. hepatica* had previously been disrupted following BI 2536 exposure [45]. However, in our hands, none of the BI 2536-treated groups exhibited reduced motility (S6B Fig). We monitored rhythmic movement (length of individual parasites plotted across frames) for subtle motility changes (S6C Fig), finding that even those treated with 10 μM BI 2536 retained the classical, 'accordion'-style movement associated with *F. hepatica* NEJs (rhythmical lengthening and shortening in a probing fashion) [135]. This was in stark contrast to treatment with 1 μM TCBZ which paralysed juveniles (S6C Fig). Our BI 2536 results are not directly comparable to those of Morawietz et al. [45] as they treated older worms (*ex vivo* immature and adults) with higher concentrations (20 μM – 100 μM).

As neoblast-like cell inhibition is associated with growth defects [20,21], worms were treated with BI 2536 for 18 h and then cultured for one week in the absence of drug. There were no significant differences between the sizes of

juveniles from any treated group and the DMSO-treated controls (Fig 6A). However, incubation of a subset of juveniles with EdU showed significantly reduced proliferation in those treated with 10 μM BI 2536 (Fig 6B; # EdU⁺ nuclei ±SEM: DMSO = 465.1 ± 109.5, 10 μM BI 2536 = 55.1 ± 25.9). A small reduction in EdU⁺ nuclei was also seen in juveniles treated with 1 μM BI 2536, though this difference was not significant. These data suggest that culture following drug exposure afforded the opportunity for flukes to recover. To test this, parasites were cultured for one week before treatment with BI 2536 and subsequent EdU exposure. These worms displayed concentration-dependent reduced cell proliferation across all groups, with significance observed at both 1 μM and 10 μM BI 2536 (Fig 6C; # EdU⁺ nuclei ±SEM: DMSO = 173.8 ± 11.5, 1 μM BI 2536 = 12.7 ± 4.7, 10 μM BI 2536 = 0 ± 0). The observed phenotypic responses are consistent with BI 2536 inhibiting PLK1 activity in *F. hepatica*, matching observations in other parasitic flatworms [40,43].

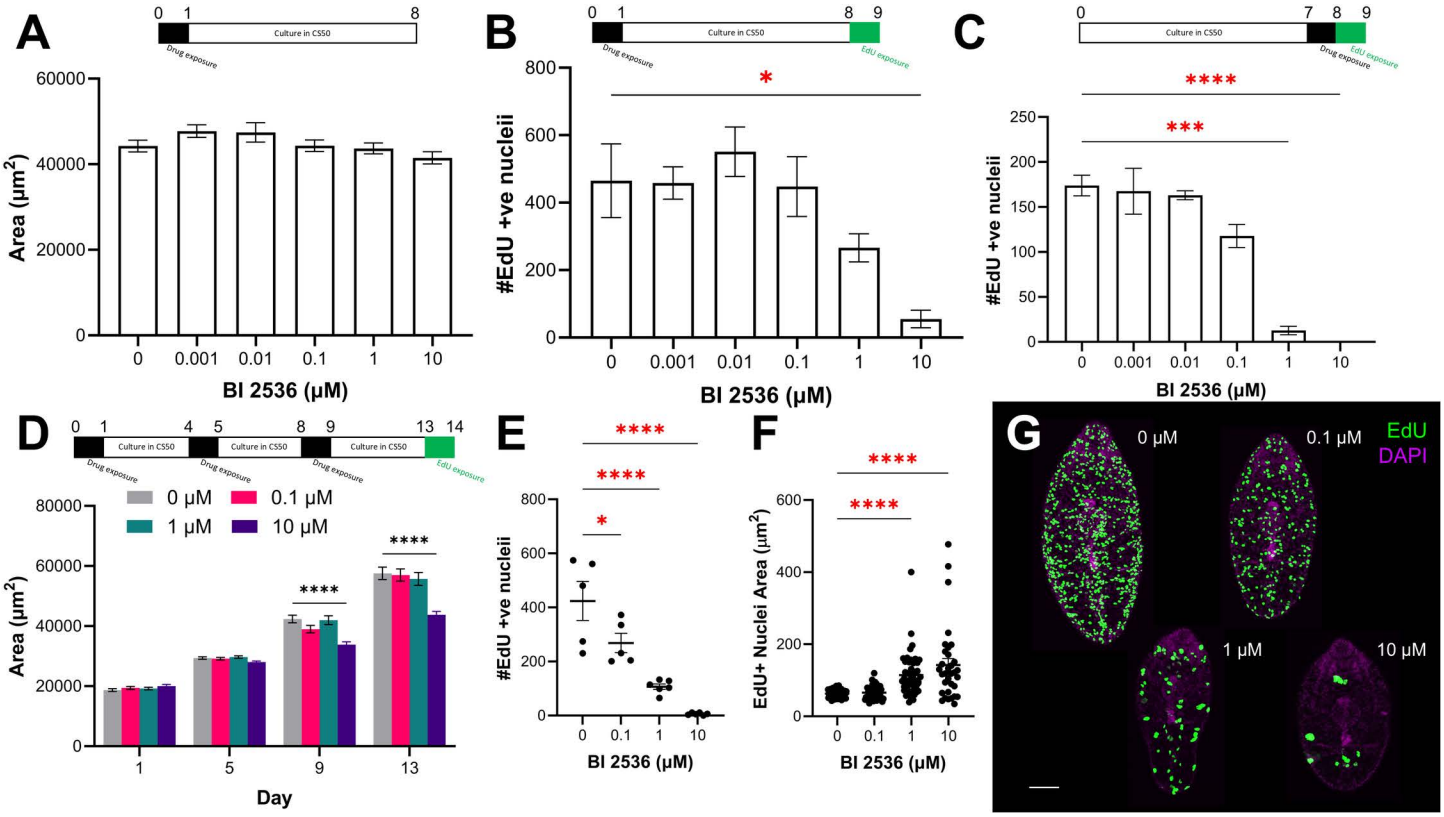


Fig 6. Repeated exposure of juvenile *Fasciola hepatica* to the PLK1 inhibitor BI 2536 *in vitro* reduces growth and proliferation. (A) Mean worm area ±SEM of 7-day-old juvenile *F. hepatica* after exposure to BI 2536 on day 0, followed by 7 days in culture, shows no effect on growth (n ≥ 39 for each treatment). **(B)** Mean # EdU⁺ nuclei ±SEM in 9-day-old *F. hepatica* after exposure to BI 2536 on day 0, followed by 8 days in culture, shows 10 μM significantly reduced the number of proliferating cells (n ≥ 7 for each treatment; Kruskal-Wallis and Dunn's posthoc tests). **(C)** Mean # EdU⁺ nuclei ±SEM in 9-day-old *F. hepatica* after exposure to BI 2536 on day 7, shows both 1 μM and 10 μM significantly reduced the number of proliferating cells (n ≥ 7 for each treatment; Kruskal-Wallis and Dunn's posthoc tests). **(D)** Mean area (μm²) ±SEM of *F. hepatica* across 13 days following BI 2536 exposures on days 0, 4 and 8 shows 10 μM significantly reduced growth rate (n ≥ 45 for each treatment at each timepoint; Kruskal-Wallis and Dunn's posthoc tests). **(E)** Mean # EdU⁺ nuclei ±SEM in 14-day-old *F. hepatica* after repeated BI 2536 exposures on days 0, 4 and 8 (timeline from **(E)** applies to this graph) shows all tested concentrations significantly reduced the number of proliferating cells (n ≥ 5 for each treatment; ANOVA and Holm-Šídák's posthoc tests). **(F)** Mean size of EdU⁺ nuclei ±SEM in 14-day-old *F. hepatica* after repeated BI 2536 exposures (1 and 10 μM) on days 0, 4 and 8 (timeline from **(E)** applies to this graph) shows increased nuclei area (n ≥ 33 for each treatment at each timepoint; Kruskal-Wallis and Dunn's posthoc tests). **(G)** Confocal images of EdU staining (green) in 14-day-old *F. hepatica* exposed to various concentrations of BI 2536 on days 0, 4 and 8 shows a dose-dependent reduction in # EdU⁺ nuclei and increase in EdU⁺ nuclei area compared to DMSO-treated control; scale bar = 100 μm, DAPI counterstain (magenta). *, p < 0.05; ***, p < 0.001; ****, p < 0.0001.

https://doi.org/10.1371/journal.ppat.1013406.g006

As BI 2536 disrupted neoblast-like cell proliferation we investigated whether it could inhibit juvenile development. For these experiments, parasites were treated with BI 2536 multiple times (on days 0, 4 and 8) with measurements taken on days 1, 5, 9 and 13. After 9 days, worms treated with 10 μM were significantly smaller than control worms (Fig 6D; day 9 mean juvenile area ±SEM: DMSO = 42368 ± 1286 μm^2, 10 μM BI 2536 = 33861 ± 907 μm^2). This phenotype was still evident following a drug-free period post treatment (Fig 6D; day 13 mean juvenile area ±SEM: DMSO = 57568 ± 2035 μm^2, 10 μM BI 2536 = 43799 ± 1122 μm^2). EdU exposure revealed significant, concentration-dependent reductions in cell proliferation across all groups (Fig 6E and 6G; # EdU$^+$ nuclei ±SEM: DMSO = 423.8 ± 72.3, 0.1 μM BI 2536 = 268.6 ± 35.5, 1 μM BI 2536 = 107 ± 10, 10 μM BI 2536 = 6 ± 1.8). These results largely phenocopy those seen following *fhplk1*-RNAi (Fig 3), supporting FhPLK1's conserved regulatory role in the proliferation of *F. hepatica* neoblast-like stem cells. We noticed that EdU$^+$ nuclei appeared larger in worms treated with higher concentrations of the drug. Therefore, we measured 10 randomly selected EdU$^+$ nuclei from five juveniles in each treatment group. This revealed that the EdU$^+$ nuclei were significantly larger in worms treated with 1 μM and 10 μM BI 2536 (Fig 6F and 6G; EdU$^+$ nuclei area: DMSO = 63.2 ± 1.6 μm^2, 1 μM BI 2536 = 114.3 ± 8.2 μm^2, 10 μM BI 2536 = 142.1 ± 18.1 μm^2). These larger nuclei could be indicative of neoblast-like cells that had passed through S phase before being delayed/arrested at either the G2/M transition or during mitosis. BI 2536 has previously been shown to increase the DNA content in cancer cells, which was attributed to an inability to undergo cytokinesis [133]. We did not observe larger EdU$^+$ nuclei throughout our RNAi experiments. This could be due to the short-term effects of inhibitor exposure which could be reversed following its removal in contrast to the long-term systemic changes to the biology of the worms throughout *fhplk1* RNAi [136].

While BI 2536 has previously been shown to affect *F. hepatica* movement *in vitro* [45], our *plk1*-RNAi and pharmacological inhibition experiments highlight how disrupting FhPLK1 activity can undermine neoblast-like cell mediated growth and development. This could weaken *F. hepatica* juveniles within the host environment, aiding parasite clearance by the immune system. BI 2536 has proven anthelmintic activity against both *S. mansoni* and *E. multilocularis*, disrupting gamete production and preventing metacestode formation from germinative cells, respectively [40,43]. Taken together, these data suggest that developing/repurposing drugs to target PLKs could be a promising anthelmintic strategy to control a range of parasitic flatworms, including different life stages.

Conclusion

This study encourages exploration of parasitic flatworm neoblast-like cells as targets for novel anthelmintics. Our annotation of the *F. hepatica* kinome showed that many kinases linked to proliferation are enriched in the highly pathogenic immature life stages. Functional genomics and inhibitor trials validated this approach as disruption of *fhplk1*, a core cell cycle-related kinase, diminished proliferation in the neoblast-like stem cell population and undermined worm growth/development. This approach could be expanded to other kinase targets such as the additional putative PLKs or the FGFRs. Indeed, the *S. mansoni* SmSAK gene has conserved roles in cell cycle progression [54], and knockdown reduced schistosomula viability *in vitro* [33]. Moreover, the ability of a kinase inhibitor to disrupt *F. hepatica* growth/development adds credence to the idea of targeting parasitic flatworm kinases [137], perhaps even in combination with current flukicides, to improve efficacy in cases of reduced drug susceptibility/resistance.

Our transcriptomic analyses highlighted possible links between *F. hepatica* neoblast-like cells and neuronal/signalling systems. Neurotransmitter signalling systems have long been touted, and exploited, as anthelmintic targets. However, if novel roles for these systems in parasitic flatworm growth/development are uncovered it opens new paths to target discovery and exploitation for drug development. A significant panel of genes were downregulated following *fhplk1*-RNAi, suggesting they have some role in mitotic regulation/stem cell biology in flukes. The work here has extended our understanding of neoblast-like cell directed growth/development in *F. hepatica* which will enhance the opportunities for novel control target discovery.

Methods

Identification of putative *F. hepatica* protein kinases

The PK sequences of the nine *Homo sapiens* ePK families, along with the aPKs, were downloaded from Uniprot (https://ftp.uniprot.org/pub/databases/uniprot/current_release/knowledgebase/complete/docs/pkinfam.txt). HMMER (v3.4; http://hmmer.org/) was used to assemble query sequences for each ePK family and the aPKs. HMM searches were carried out using HMMER against the University of Liverpool and Washington University *F. hepatica* predicted proteomes [47,138] downloaded from Wormbase ParaSite (WBPS19, https://parasite.wormbase.org) [139]. We also looked for additional kinases in a set of novel transcripts. These were generated by aligning all publicly available *F. hepatica* transcriptomic reads [21,46,47] and in-house transcriptomic datasets against the University of Liverpool genome (WBPS19, https://parasite.wormbase.org/Fasciola_hepatica_prjeb58756/Info/Index/) using HISAT2 (v.2.1.0), before transcript assembly with Stringtie (v1.3.6) to create a master reference gtf file containing 14,684 'novel' transcripts that did not overlap with genes in the reference assembly. All putative hits were screened via BLAST searches against the SwissProt database, and domains annotated using InterPro (https://www.ebi.ac.uk/interpro/about/interproscan/). Hits were retained only when the top BLAST result was a PK, and when a kinase domain was predicted to be present. Duplicates/putative gene copies were identified using Clustal Omega (https://www.ebi.ac.uk/Tools/msa/clustalo/) and manually inspected before removal. The remaining putative *F. hepatica* PKs were used to create two HMM query sequences (one ePK and one aPK) which were then used in further HMM searches against both *F. hepatica* predicted proteomes [47,138] to ensure no PKs were missed. Resulting hits were sorted through the same pipeline. BLAST results were used to classify which family/subfamily putative *F. hepatica* kinases belonged to.

Putative ePKs were clustered using CLANs analysis software (1,000,000 rounds of clustering; [140]). MEGA11 (https://megasoftware.net/, [141]) was used to align aPKs (ClustalW), identify the optimum model for phylogenetic analysis, and construct a Maximum Likelihood (ML) tree with 500 bootstraps. This ML tree was visualised using the Interactive Tree of Life (https://itol.embl.de/).

Published life-stage transcriptomic data from eggs, metacercariae, 1 h newly excysted juveniles (NEJs), 3 h NEJs, 24 h NEJs, three-week juveniles and adults [47] were used to obtain median TPM values for all predicted PKs. Z scores were generated, and heatmaps produced using Morpheus software (https://software.broadinstitute.org/morpheus).

F. hepatica in vitro excystment and culture

The Italian strain of *F. hepatica* (Ridgeway Research, UK) was used for all experiments. Excystments were carried out as previously described [88,142], and a detailed protocol is available at https://dx.doi.org/10.17504/protocols.io.14egn-212qg5d/v1. Briefly, metacercariae were physically 'popped' from their outer cyst walls and treated with 10% (v/v) sodium hypochlorite (#1056142500, Sigma-Aldrich) diluted in double-distilled water (ddH_2O) for 2–3 minutes (exact time dependent on metacercariae batch). Popped and bleached metacercariae were then washed in ddH_2O at least five times to remove excess sodium hypochlorite, prior to being stimulated to excyst as detailed by McVeigh et al. [142]. Parasites were cultured in 200 µL CS50 (50% (v/v) chicken serum (#16110082, Thermo Fisher Scientific) in RPMI (#11835105, Thermo Fisher Scientific) with antibiotic/antimycotic (#A5955, Sigma Aldrich)) in 96-well, round-bottomed plates (#83.3925, Sarstedt) in a humidified incubator at 37°C with 5% CO_2 as previously described [20]. Media changes were performed three times per week. *F. hepatica* in culture media are referred to as juveniles.

RNAi of *fhplk1 in vitro*

We generated cDNA from four-week-old juvenile *F. hepatica* by snap freezing 20 juveniles in liquid N_2. Tissues were lysed in a Qiagen tissue lyser with a stainless-steel bead (50 oscillations/sec for 1 min) prior to mRNA extraction with the Dynabeads mRNA Direct Purification Kit (#61011, Thermo Fisher Scientific), DNase treatment (Turbo DNA-free

Kit, # AM1907, Thermo Fisher Scientific) and reverse transcription to cDNA using the High-Capacity RNA-to-cDNA Kit (#4387406, Thermo Fisher Scientific). All cDNAs were diluted 1:1 in ddH_2O prior to use. Double-stranded (ds)RNA templates specific to *fhplk1* (FhHiC23_g6132) were generated using 0.4 μM T7-labelled primers (5'-TAATACGACTCACTATAGGGT-3') and the FastStart Taq DNA Polymerase, dNTPack (#4738357001, Millipore Sigma). Primers were designed using Primer3Plus [143], and amplicons were sequenced by Eurofins Genomics (https://eurofinsgenomics.eu/en/) to ensure target specificity. Primers used to generate *fhplk1*-specific dsRNA templates can be found in S10 Table. Negative control dsRNA targeting bacterial neomycin phosphotransferase [U55762] was generated as previously detailed [142]. Template sizes were checked on a 1–2% agarose gel prior to purification using the ChargeSwitch PCR Clean-Up Kit (#CS12000, Thermo Fisher Scientific) and dsRNA generation using the T7 RiboMAX Express RNA System (#P1700, Promega). All dsRNAs were resuspended in ddH_2O with concentrations/purities checked on a DeNovix DS-11 FX spectrophotometer prior to storage as single-use aliquots at -20°C. RNAi treatments were performed by soaking worms in 50 μL of 100 ng/μL dsRNA diluted in RPMI for 24 h in 96-well round-bottomed plates under standard conditions detailed above. NEJs were immediately exposed to target-specific dsRNA with juveniles subsequently treated twice a week across four weeks to ensure knockdown [88]. Juveniles were cultured in CS50 between RNAi treatments as standard. All RNAi experiments were carried out in triplicate and included no dsRNA-treatment controls.

Juveniles were imaged each week by capturing darkfield videos/images on an Olympus SC50 camera attached to an Olympus SZX10 microscope. Video analyses were performed using the wrMTrck plugin (http://www.phage.dk/plugins/wrmtrck.html, [144]) for ImageJ calibrated to a 1 mm scale. The wrMTrck plugin was used as default except for modifications to minSize (10 pixels), maxSize (1000 pixels), maxVelocity (1000 pixels/frame), AreaChange (200% change in area between frames), Rawdata (2) and benddetect (0). Motility was measured by calculating changes in juvenile length between frames, which provided length change (μm)/minute. Movement of individual juveniles were normalised against mean movement of control juveniles. wrMTrck also provided area (μm^2) measurements for each worm.

At the conclusion of RNAi trials juveniles were frozen in liquid N_2 in batches of 20 worms/replicate before cDNA extraction as described above. Quantification of target transcript knockdown was carried out on a Qiagen RotorGene Q 5-plex HRM instrument under the following running conditions: 95°C for 10 minutes; 40 cycles @ 95°C for 10 sec, 55°C for 15 sec and 72°C for 20 sec. Melt-curve analyses were enabled to confirm product specificity and qPCR reactions were performed in triplicate using the SensiFast SBYR No-ROX kit (#BIO-98005, Bioline) with final primer concentrations of 200 nM. Glyceraldehyde phosphate dehydrogenase (*fhgapdh*) [AY005475] was used as a housekeeper gene. Alongside *fhplk1*, *fhh2b* [D915_007751] and *fhmlc* [FhHiC23_g308] were amplified as markers for proliferating cells and muscle cells respectively. The oligonucleotide primers used can be found in S10 Table. Pfaffl's Augmented ΔΔCt method [145] was used to calculate relative gene expression. Transcript expression was plotted for both target and control-dsRNA-treated groups relative to no dsRNA control.

Visualisation of proliferative cell activity

The thymidine analogue, EdU (Thermo Fisher Scientific) was used to label nuclei of proliferating neoblast-like cells. A 10 mM stock of EdU was stored at -20°C in PBS. Stock solution was diluted in CS50 to a final working concentration of 500 μM and placed on juveniles for 24 h under standard culture conditions. Immediately following EdU exposure worms were flat-fixed under a coverslip in 4% paraformaldehyde (w/v) in PBS (PFA) for 15 minutes, prior to a further 4 h free-fixing in 4% PFA at room temperature while constantly rotating. Worms were permeabilised in 0.5% Triton X-100 in PBS for 30 min at room temperature. EdU detection was achieved using the Click-iT EdU Proliferation Kit for Imaging with the Alexa Fluor 488 dye (#C10337, Thermo Fisher Scientific). Worms were counterstained using 4′,6-diamidino-2-phenylindole (#D1306, DAPI) in PBS for 20 minutes at room temperature prior to mounting in Vectashield (#H-1000–10, Vector Laboratories). A detailed protocol is available at https://dx.doi.org/10.17504/protocols.io.eq2lyjnrrlx9/v1.

Samples were imaged on a Leica TCS SP8 inverted microscope. Z-stacks consisting of 10–15 optical sections between the dorsal and ventral surfaces were captured for each worm and maximally projected for analyses. EdU^+ nuclei counts were performed using the cell counter plugin for ImageJ (https://imagej.nih.gov/ij/plugins/cell-counter.html). Nuclei area (μm^2) measurements were also performed in ImageJ, where images were calibrated to a 50 μm scale.

RNA-seq and miRNA-seq of *fhplk1* RNAi *F. hepatica* juveniles

NEJs were excysted and treated with target-specific dsRNA as described above (~50 worms/replicate split across two wells). Three replicates for each treatment were carried out in total. Juveniles were treated with dsRNA in RPMI for the final time on day 21 before being snap frozen in liquid N_2 the following day and stored at -80°C. Total RNA was extracted using Trizol reagent (#15596026, Thermo Fisher Scientific) before being sent to the Genomics Core Technology Unit at Queen's University Belfast (https://www.qub.ac.uk/sites/core-technology-units/Genomics/) for RNA quantification/purity assessment on an AATI fragment analyser prior to library generation using the KAPA mRNA HyperPrep Kit (#KK8580, Roche). Libraries were sequenced (paired end, 2 x 50 bp) on an Illumina Nova seq 6000 SP100 with ~50M reads/sample. Raw read files were uploaded to the European Nucleotide Archive and are available under accession PRJEB85227. Read quality was assessed by fastqc (v.0.11.8) prior to read alignment via HISAT2 (v.2.1.0) against the University of Liverpool *F. hepatica* genome [47] using genome and GTF files available on Wormbase ParaSite (WBPS19, https://parasite.wormbase.org/Fasciola_hepatica_prjeb58756/Info/Index/). Transcripts were assembled in Stringtie (v1.3.6) and a master reference file, excluding isoforms, was generated by merging transcripts from different replicates with the reference genome. This master reference file was used to generate gene counts via Stringtie (v1.3.6) before export into a format readable by DESeq2. 'Novel' transcripts (MSTRGs) generated by Stringtie (v1.3.6) can be found in S2 File.

'Novel' MSTRG sequences with no BLAST hit in the NCBI nr database other than *F. hepatica* and genes with <10 counts across all samples were removed before differential gene expression analysis in R (v4.2.1) by DESeq2 (v.1.34.0). A p-value threshold of 0.001 false discovery rate (FDR) was set to identify differentially expressed genes (DEGs). These DEGs were annotated using the OmicsBox BLAST2GO suite [146] via BLASTx searches against the NCBI non-redundant, landmark and SwissProt databases. Additional BLASTs were carried out against the *S. mansoni* genome (v10, WBPS19, https://parasite.wormbase.org/Schistosoma_mansoni_prjea36577/Info/Index/). Gene ontology (GO) terms were mapped to genes based on BLAST searches and InterproScan results by BLAST2GO annotation software [146] before TOPGO (v.2.36) analysis (parameters: FDR < 0.05, method = weight01, statistic = fisher) was carried out on DEGs. KEGG IDs were assigned to transcripts using the eggNOG-mapper [147] tool in OmicsBox (https://www.biobam.com/omicsbox) before gage (v.2.44) and pathview (v.1.34) were used to identify up and downregulated pathways. TOPGO (v.2.36) analysis of *S. mansoni* upregulated genes from Collins et al. [13] was performed by updating all genes to their current IDs and downloading GO terms from Wormbase ParaSite (WBPS19). Parameters were as those used for *F. hepatica* TOPGO analysis. R scripts are available on Github (https://github.com/pmccusker09/F.hepatica_plk1-RNAi_transcriptome_R_analysis.git).

Remaining total RNA was processed by the Genomics Core Technology Unit at Queen's University Belfast for miRNA sequencing. Briefly, total RNA was library prepped with the QIASeq miRNA prep kit (#331502, Qiagen) and sequenced on an Illumina Next Seq 2000 with ~8 M single reads per sample (100 bp). Adaptor sequences were trimmed using trimgalore (v.0.4.4) and read quality was assessed by fastqc (v.0.11.8). Raw read files are available under accession PRJEB85228 at the European Nucleotide Archive. Reads were mapped to the University of Liverpool genome downloaded from WormBase ParaSite (WBPS18, https://parasite.wormbase.org/Fasciola_hepatica_prjeb25283/Info/Index/) by bowtie2 (v.2.3.5.1) and miRDeep2 (v.0.1.3) before miRNA counts were generated by miRDeep2 (v.0.1.3), using predicted mature *F. hepatica* miRNAs [131] as a guide. Only counts that mapped to miRNAs previously identified by Herron et al. [131] were taken forward for differential expression analysis by DESeq2 (v.1.34.0) in R (v4.2.1). The targets of differentially expressed miRNAs were predicted by using the same thresholds as Gillan et al. [148]; miRanda (v.; total score >145, energy < -10),

RNAhybrid (v.; p < 0.1, energy < -22) and PITA (v.; seed sequence of 8 bases with DDG < -10). Target prediction was based on the WBPS18 version of the *F. hepatica* genome, as the miRNAs were predicted from that assembly [131], and so RNA-seq analysis was also carried out against this previous version of the genome assembly using the same methodology as detailed above.

Exposure of juvenile *F. hepatica* to PLK1 inhibitor *in vitro*

The PLK inhibitor, BI 2536 (Millipore Sigma) was chosen for testing on juvenile *F. hepatica in vitro*. BI 2536 has a strong selectivity for PLK1 and so the amino acid sequence of FhPLK1 was examined to determine if key amino acid residues implicated in drug binding were conserved [132]. The PLK1 sequences of *F. hepatica*, *H. sapiens* [P53350], *S. mansoni* [Q5UES2] and *E. multilocularis* [U6HQM1], were aligned using Clustal Omega (https://www.ebi.ac.uk/Tools/msa/clustalo/). Other putative *F. hepatica* PLKs identified in our bioinformatic screen were included in the alignment to help predict BI 2536 activity. Further BLAST searches against the *F. hepatica* predicted proteomes (WBPS19, https://parasite.wormbase.org) with *H. sapiens* PLKs1-5 [P53350; Q9NYY3; Q9H4B4; O00444; Q496M5] as query sequences did not identify additional *F. hepatica* PLKs.

BI 2536 (#A10134, AdooQ Bioscience) and TCBZ (#1681611, Millipore Sigma) were dissolved in 1.7 mL NoStick hydrophobic microtubes (#1210-S0, SSIbio) using dimethyl sulphoxide (DMSO). Juvenile *F. hepatica* were washed three times in 1 mL RPMI 1640 to remove excess CS50. They were then transferred to 3.5 cm petri dishes (#82.1135.500, Sarstedt) for exposure in up to 10 μM test compound in a final volume of 3 mL RPMI 1640 for 18 h in standard culture conditions. Compounds were added such that the final DMSO concentration was 0.1% (v/v) in 3 mL RPMI. A vehicle control group (DMSO-treated) was included, with treatments carried out in triplicate. At the conclusion of drug incubations juveniles were subjected to phenotypic observation as detailed above. Where NEJs/juveniles were being further cultured post-exposure, they were washed three times in 1 mL RPMI 1640 to remove excess drug, prior to further culturing as previously described.

Statistical analyses

Unless otherwise stated graphs were generated and statistical analyses performed in GraphPad Prism (v10, La Jolla, CA USA). All datasets were tested for normality using either Kolmogorov-Smirnov or Shapiro-Wilk tests. Where data were normally distributed, parametric tests were performed, whereas nonparametric tests were employed where data were non-normally distributed. Relevant post-hoc tests (e.g. Dunn's, Dunnett's and Tukey's multiple comparisons tests) were performed to identify significant differences between multiple groups. Volcano plots were produced using R (v4.2.1). Mean ±standard error mean (SEM) is displayed on graphs unless otherwise stated. Raw data used to generate figures can be found in S11 Table.

Supporting information

S1 Fig. *Fasciola hepatica* protein kinases are enriched in developing life stages. (A) Bioinformatics pipeline used to identify putative protein kinases in *F. hepatica* through HMM searches, BLAST identification, manual curation and CLANs analysis. (B) Proportions (%) of eukaryotic protein kinase families in *F. hepatica*, *Schistosoma mansoni*, *Schistosoma haematobium*, *Caenorhabditis elegans*, *Haemonchus contortus*, *Drosophila melanogaster* and *Homo sapiens* kinomes. (C) Maximum-likelihood tree (WAG + G + F model) with 100 bootstraps of predicted *F. hepatica* atypical protein kinases; colours denote family. (D) Heatmap of *F. hepatica* kinases (where data were available from WormBase ParaSite) in eggs, metacercariae, 1 h Newly excysted juveniles (NEJs) *in vitro*,3 h Newly excysted juveniles (NEJs) *in vitro*, 24 h Newly excysted juveniles (NEJs) *in vitro*, 3-week immature juveniles *in vivo* and adults (Left) with average Euclidean distancing applied shows increased expression of many kinases in NEJs and immature worms. The expression of these kinase genes was also compared between *in vivo* juvenile and *in vitro* juveniles (Right, [46]) showing increased expression of

many kinases in faster growing *in vivo* juveniles; colours correspond to z scores (red = upregulated; blue = downregulated; grey = no change; black = no expression data).
(TIF)

S2 Fig. Cell proliferation does not recover up to a week after *fhplk1* dsRNA exposure in juvenile *Fasciola hepatica* *in vitro*. (A) Timelines for experiments show juvenile *F. hepatica* were treated for four weeks with either control dsRNA or *fhplk1* dsRNA before a final week in culture with no dsRNA treatments prior to EdU exposure and subsequent staining. (B) Confocal images of EdU staining (green) in juvenile *F. hepatica* treated according to adjacent timelines show that EdU^+ nuclei did not recover after *fhplk1* dsRNA exposures were stopped; scale bar = 100 μm, DAPI counterstain (magenta). (C) Mean # EdU^+ nuclei ±SEM in juvenile *F. hepatica* treated according to adjacent timelines shows complete loss of EdU^+ nuclei in *fhplk1* dsRNA-treated worms, even after culture for one week post drug exposure ($n \geq 8$ for each treatment; Mann-Whitney U test). Experimental timelines schematic created in BioRender.
(TIF)

S3 Fig. Downregulation of cell cycle and ribosome associated transcripts in *fhplk1*-RNAi juvenile *Fasciola hepatica*. (A) Mean area (μm^2) ±SEM of juvenile *F. hepatica* used in transcriptomics shows reduced growth rate in worms repeatedly treated with *fhplk1* dsRNA for three weeks ($n \geq 141$ for each treatment; Mann-Whitney U test). (B) Confocal images of EdU staining (green) in juvenile *F. hepatica* used for transcriptomics confirmed ablation of EdU^+ nuclei after repeated treatment with *fhplk1* dsRNA for three weeks. (C) GO terms (top 10 molecular function and top 10 cellular component) overrepresented among downregulated transcripts following *fhplk1* dsRNA treatment in juvenile *F. hepatica*. (D) KEGG pathways significantly downregulated following *fhplk1*-RNAi in juvenile *F. hepatica* are associated with ribosomal components and cell cycle/proliferation. (E) Integrative genomics viewer (IGV) screenshot of transcriptomic reads in all RNA sequenced samples mapped against the *F. hepatica fhplk1* gene shows reads across the whole gene in control dsRNA samples, but a spike in reads around the dsRNA amplicon region in *fhplk1* dsRNA samples (red box to highlight). (F) IGV screenshots of beginning and end of *fhplk1* dsRNA amplicon region show that reads in *fhplk1* dsRNA samples begin and end where forward ('F' green) and reverse ('R' pink) amplicon primers are located.
(TIF)

S4 Fig. Upregulated cell signalling and receptors/ion channel subunits in *fhplk1*-RNAi *Fasciola hepatica* juveniles. (A) GO terms (top 10 molecular function and top 10 cellular component) overrepresented in transcripts upregulated following *fhplk1*-RNAi in *F. hepatica* juveniles. (B) KEGG pathways associated with inter-cell signalling (gap junction, neural synapses and signalling pathways) significantly upregulated following *fhplk1*-RNAi in juvenile *F. hepatica*. (C) KEGG Gap Junction pathway following *fhplk1*-RNAi shows upregulation of diverse pathway components (red = upregulated; grey = no change; blue = downregulated; white = unassigned KEGG ID). (D) KEGG serotonergic synapse pathway following *fhplk1*-RNAi shows upregulation of diverse pathway components (red = upregulated; grey = no change; blue = downregulated; white = unassigned KEGG ID). (E) Top 10 Biological process GO terms overrepresented in significantly upregulated transcripts in both *fhplk1*-RNAi and slower growing *in vitro* worms (S6 Table) are associated with neuronal signalling. (F) DAPI (nuclei) stain coverage (as a percentage of the total area of the worm) in control-dsRNA treated and *fhplk1*-dsRNA treated worms shows ~20% reduction ($n \geq 3$ for each treatment). (G) Significantly upregulated receptors/channel subunits following *fhplk1*-RNAi.
(TIF)

S5 Fig. GO terms of predicted targets for differentially expressed miRNAs following *fhplk1*-RNAi in *Fasciola hepatica* juveniles do not match the GO terms associated with differentially expressed mRNAs. (A) Volcano plot of miRNA expression (red dots indicate differentially expressed miRNA) in *fhplk1*-RNAi juvenile *F. hepatica*. (B) Mean $\log_2$foldchange and frequency of GO terms for the predicted target transcripts of differentially expressed miRNAs following *fhplk1*-RNAi in *F. hepatica* juveniles.
(TIF)

S6 Fig. The PLK1 inhibitor BI 2536 does not affect *Fasciola hepatica* motility *in vitro*. (A) Conservation of BI 2536 binding residues within *F. hepatica* FhPLK1, *Echinococcus multilocularis* EmPLK1, *Schistosoma mansoni* SmPLK1 and *Homo sapiens* PLK1 kinase domains, but not FhPLK2 or FhPLK4 (residues implicated in BI 2536 binding highlighted in black; Leu_{132} residue critical to drug interaction in *H. sapiens* PLK1 highlighted in red and marked with a red arrow). (B) Worm motility (%) ±SEM of *F. hepatica* newly excysted juveniles (NEJs) 18 hours after *in vitro* BI 2536 treatment ($n \geq 49$ for each treatment). (C) Motility profile of *F. hepatica* NEJs treated with 10 μM BI 2536 (blue), 0.1% DMSO (purple) and 1 μM TCBZ (green). Each line represents a single parasite; data presented as worm length (μm) over time (frames).
(TIF)

S1 Table. Summary table of predicated *Fasciola hepatica* kinome based on bioinformatic screen. Genes IDs, BLAST hits, IDs in alternative *F. hepatica* genome assembly listed. Eukaryotic protein kinases and atypical protein kinases in separate sheets.
(XLSX)

S2 Table. Summary of kinases downregulated following irradiation of *Fasciola hepatica* juveniles and upregulated in faster-growing *in vivo F. hepatica* juveniles.
(XLSX)

S3 Table. DESeq2 results after three weeks of *fhplk1* RNAi in *Fasciola hepatica* juveniles *in vitro*. (Sheet 1) Downregulated genes (adjp < 0.001), (Sheet 2) Upregulated genes (adjp < 0.001), (Sheet 3) All DESeq2 results.
(XLSX)

S4 Table. Common downregulated genes following *fhplk1* RNAi in *Fasciola hepatica* juveniles, irradiation in *F. hepatica* juveniles and irradiation in *Schistosoma mansoni* adults. (Sheet 1) Genes downregulated in both *fhplk1*-RNAi-*F. hepatica* juveniles, irradiated *F. hepatica* juveniles and irradiated *S. mansoni* adults. (Sheet 2) Genes downregulated in both irradiated *F. hepatica* juveniles and irradiated *S. mansoni* adults. (Sheet 3) Genes downregulated in both *fhplk1*-RNAi-*F. hepatica* juveniles and irradiated *S. mansoni* adults. (Sheet 4) Genes downregulated in both *fhplk1*-RNAi-*F. hepatica* juveniles and irradiated *F. hepatica* juveniles.
(XLSX)

S5 Table. Log_2FoldChange of predicted *Fasciola hepatica* neuropeptides following RNAi of *fhplk1* in juveniles across three weeks *in vitro*.
(XLSX)

S6 Table. Shared genes that are upregulated following *fhplk1* RNAi and downregulated in faster-growing *in vivo F. hepatica* juveniles.
(XLSX)

S7 Table. Comparison of fold change for signalling-associated genes following *fhplk1* RNAi or in faster-growing *in vivo F. hepatica* juveniles.
(XLSX)

S8 Table. GO terms upregulated in adult *Schistosoma mansoni* following neoblast-like cell ablation. (Sheet 1) GO terms upregulated 14 days after irradiation. (Sheet 2) GO terms upregulated 21 days after *smh2b* RNAi. (Sheet 3) GO terms upregulated 21 days after *smfgfrA* RNAi.
(XLSX)

S9 Table. Differentially expressed miRNAs following *fhplk1* RNAi in *Fasciola hepatica* juveniles. (Sheet 1) Differentially expressed miRNAs. (Sheet 2) Predicted targets of differentially expressed miRNAs.
(XLSX)

S10 Table. Primers used in PCR reactions.
(XLSX)

S11 Table. Raw values used to produce graphs in Figs 1, 3–6, S1–S4 and S6.
(XLSX)

S1 File. Fasta file of all sequences in predicted *Fasciola hepatica* kinome.
(TXT)

S2 File. Nucleotide sequences of 'novel' MSTRG *Fasciola hepatica* transcripts identified by Stringtie during transcriptomic processing.
(FASTA)

Author contributions

Conceptualization: Paul McCusker, Nathan G. Clarke, John Harrington, Paul M. Selzer, Nikki J. Marks, Aaron G. Maule.

Data curation: Paul McCusker, Nathan G. Clarke, Rebecca Armstrong, Duncan Wells, Paul McVeigh, Aaron G. Maule.

Formal analysis: Paul McCusker, Nathan G. Clarke, Emily Robb, Paul McVeigh, Nikki J. Marks, Aaron G. Maule.

Funding acquisition: John Harrington, Paul M. Selzer, Nikki J. Marks, Aaron G. Maule.

Investigation: Paul McCusker, Nathan G. Clarke, Rebecca Armstrong.

Methodology: Paul McCusker, Nathan G. Clarke, Rebecca Armstrong.

Project administration: Nikki J. Marks, Aaron G. Maule.

Resources: Paul McCusker.

Supervision: Nikki J. Marks, Aaron G. Maule.

Visualization: Paul McCusker, Nathan G. Clarke, Duncan Wells, Emily Robb, Aaron G. Maule.

Writing – original draft: Paul McCusker, Aaron G. Maule.

Writing – review & editing: Paul McCusker, Nathan G. Clarke, Rebecca Armstrong, Duncan Wells, Emily Robb, Paul McVeigh, Andreas Krasky, John Harrington, Paul M. Selzer, Nikki J. Marks, Aaron G. Maule.

References

1. FAO. Diseases in domestic animals caused by flukes. Rome: Food and Agriculture Organisation of the United Nations; 1994.
2. WHO. Integrating neglected tropical diseases into global health and development: fourth WHO report on neglected tropical diseases. Geneva; 2017. Available from: https://unitingtocombatntds.org/wp-content/uploads/2017/11/4th_who_ntd_report.pdf
3. Kelley JM, Elliott TP, Beddoe T, Anderson G, Skuce P, Spithill TW. Current Threat of Triclabendazole Resistance in *Fasciola hepatica*. Trends Parasitol. 2016;32(6):458–69. https://doi.org/10.1016/j.pt.2016.03.002 PMID: 27049013
4. McVeigh P, McCusker P, Robb E, Wells D, Gardiner E, Mousley A, et al. Reasons to Be Nervous about Flukicide Discovery. Trends Parasitol. 2018;34(3):184–96. https://doi.org/10.1016/j.pt.2017.11.010 PMID: 29269027
5. Boray JC. Studies on experimental infections with *Fasciola hepatica*, with particular reference to acute fascioliasis in sheep. Ann Trop Med Parasitol. 1967;61(4):439–50. https://doi.org/10.1080/00034983.1967.11686513 PMID: 5634134
6. Fairweather I, Boray JC. Fasciolicides: efficacy, actions, resistance and its management. Vet J. 1999;158(2):81–112. https://doi.org/10.1053/tvjl.1999.0377 PMID: 10489266
7. Wagner DE, Wang IE, Reddien PW. Clonogenic neoblasts are pluripotent adult stem cells that underlie planarian regeneration. Science. 2011;332(6031):811–6. https://doi.org/10.1126/science.1203983 PMID: 21566185
8. Wolff E, Dubois F. Sur la migration des cellules de régénération chez les Planaires. Revue suisse de zoologie. 1948;55:218–27. https://doi.org/10.5962/bhl.part.117877
9. Campbell NJ, Gregg P, Kelly JD, Dineen JK. Failure to induce homologous immunity to *Fasciola hepatica* in sheep vaccinated with irradiated metacercariae. Veterinary Parasitology. 1978;4(2):143–52. https://doi.org/10.1016/0304-4017(78)90005-5

10. Creaney J, Spithill TW, Thompson CM, Wilson LR, Sandeman RM, Parsons JC. Attempted immunisation of sheep against *Fasciola hepatica* using gamma-irradiated metacercariae. Int J Parasitol. 1995;25(7):853–6. https://doi.org/10.1016/0020-7519(94)00204-2 PMID: 7558572
11. Wang B, Collins JJ 3rd, Newmark PA. Functional genomic characterization of neoblast-like stem cells in larval Schistosoma mansoni. Elife. 2013;2:e00768. https://doi.org/10.7554/eLife.00768 PMID: 23908765
12. Collins JJ 3rd, Wang B, Lambrus BG, Tharp ME, Iyer H, Newmark PA. Adult somatic stem cells in the human parasite Schistosoma mansoni. Nature. 2013;494(7438):476–9. https://doi.org/10.1038/nature11924 PMID: 23426263
13. Collins JJ 3rd, Wendt GR, Iyer H, Newmark PA. Stem cell progeny contribute to the schistosome host-parasite interface. Elife. 2016;5:e12473. https://doi.org/10.7554/eLife.12473 PMID: 27003592
14. Wendt GR, Collins JN, Pei J, Pearson MS, Bennett HM, Loukas A, et al. Flatworm-specific transcriptional regulators promote the specification of tegumental progenitors in Schistosoma mansoni. Elife. 2018;7:e33221. https://doi.org/10.7554/eLife.33221 PMID: 29557781
15. Koziol U, Rauschendorfer T, Zanon Rodríguez L, Krohne G, Brehm K. The unique stem cell system of the immortal larva of the human parasite Echinococcus multilocularis. Evodevo. 2014;5(1):10. https://doi.org/10.1186/2041-9139-5-10 PMID: 24602211
16. Rozario T, Quinn EB, Wang J, Davis RE, Newmark PA. Region-specific regulation of stem cell-driven regeneration in tapeworms. Elife. 2019;8:e48958. https://doi.org/10.7554/eLife.48958 PMID: 31549962
17. Collins JNR, Collins JJ 3rd. Tissue Degeneration following Loss of Schistosoma mansoni cbp1 Is Associated with Increased Stem Cell Proliferation and Parasite Death In Vivo. PLoS Pathog. 2016;12(11):e1005963. https://doi.org/10.1371/journal.ppat.1005963 PMID: 27812220
18. Wendt G, Shiroor DA, Adler CE, Collins JJ III. Convergent evolution of "genome guardian" functions in a parasite-specific p53 homolog. bioRxiv. 2021; 2021.11.28.470261. https://doi.org/10.1101/2021.11.28.470261
19. Romero AA, Cobb SA, Collins JNR, Kliewer SA, Mangelsdorf DJ, Collins JJ III. The *Schistosoma mansoni* nuclear receptor FTZ-F1 maintains esophageal gland function via transcriptional regulation of meg-8.3. PLoS Pathog. 2021;17:e1010140. https://doi.org/10.1371/journal.ppat.1010140
20. McCusker P, McVeigh P, Rathinasamy V, Toet H, McCammick E, O'Connor A, et al. Stimulating Neoblast-Like Cell Proliferation in Juvenile *Fasciola hepatica* Supports Growth and Progression towards the Adult Phenotype In Vitro. PLoS Negl Trop Dis. 2016;10(9):e0004994. https://doi.org/10.1371/journal.pntd.0004994 PMID: 27622752
21. McCusker P, Clarke NG, Gardiner E, Armstrong R, McCammick EM, McVeigh P, et al. Neoblast-like stem cells of *Fasciola hepatica*. PLoS Pathog. 2024;20(5):e1011903. https://doi.org/10.1371/journal.ppat.1011903 PMID: 38805551
22. Fabbro D, Cowan-Jacob SW, Moebitz H. Ten things you should know about protein kinases: IUPHAR Review 14. Br J Pharmacol. 2015;172(11):2675–700. https://doi.org/10.1111/bph.13096 PMID: 25630872
23. Manning G, Whyte DB, Martinez R, Hunter T, Sudarsanam S. The protein kinase complement of the human genome. Science. 2002;298(5600):1912–34. https://doi.org/10.1126/science.1075762 PMID: 12471243
24. Sharma K, D'Souza RCJ, Tyanova S, Schaab C, Wiśniewski JR, Cox J, et al. Ultradeep human phosphoproteome reveals a distinct regulatory nature of Tyr and Ser/Thr-based signaling. Cell Rep. 2014;8(5):1583–94. https://doi.org/10.1016/j.celrep.2014.07.036 PMID: 25159151
25. Wilson LJ, Linley A, Hammond DE, Hood FE, Coulson JM, MacEwan DJ, et al. New Perspectives, Opportunities, and Challenges in Exploring the Human Protein Kinome. Cancer Res. 2018;78(1):15–29. https://doi.org/10.1158/0008-5472.CAN-17-2291 PMID: 29254998
26. Roskoski R Jr. Properties of FDA-approved small molecule protein kinase inhibitors. Pharmacol Res. 2019;144:19–50. https://doi.org/10.1016/j.phrs.2019.03.006 PMID: 30877063
27. Gramberg S, Puckelwaldt O, Schmitt T, Lu Z, Haeberlein S. Spatial transcriptomics of a parasitic flatworm provides a molecular map of drug targets and drug resistance genes. Nat Commun. 2024;15(1):8918. https://doi.org/10.1038/s41467-024-53215-3 PMID: 39414795
28. Grevelding CG, Langner S, Dissous C. Kinases: Molecular Stage Directors for Schistosome Development and Differentiation. Trends Parasitol. 2018;34(3):246–60. https://doi.org/10.1016/j.pt.2017.12.001 PMID: 29276074
29. Arora N, Raj A, Anjum F, Kaur R, Rawat SS, Kumar R, et al. Unveiling Taenia solium kinome profile and its potential for new therapeutic targets. Expert Rev Proteomics. 2020;17(1):85–94. https://doi.org/10.1080/14789450.2020.1719835 PMID: 31968176
30. Stroehlein AJ, Young ND, Jex AR, Sternberg PW, Tan P, Boag PR, et al. Defining the Schistosoma haematobium kinome enables the prediction of essential kinases as anti-schistosome drug targets. Sci Rep. 2015;5:17759. https://doi.org/10.1038/srep17759 PMID: 26635209
31. Andrade LF, Nahum LA, Avelar LGA, Silva LL, Zerlotini A, Ruiz JC, et al. Eukaryotic protein kinases (ePKs) of the helminth parasite Schistosoma mansoni. BMC Genomics. 2011;12:215. https://doi.org/10.1186/1471-2164-12-215 PMID: 21548963
32. Sarkar N, Singh A, Kumar P, Kaushik M. Protein kinases: Role of their dysregulation in carcinogenesis, identification and inhibition. Drug Res (Stuttg). 2023;73(4):189–99. https://doi.org/10.1055/a-1989-1856 PMID: 36822216
33. Llamazares S, Moreira A, Tavares A, Girdham C, Spruce BA, Gonzalez C, et al. polo encodes a protein kinase homolog required for mitosis in Drosophila. Genes Dev. 1991;5(12A):2153–65. https://doi.org/10.1101/gad.5.12a.2153 PMID: 1660828
34. Sunkel CE, Glover DM. polo, a mitotic mutant of Drosophila displaying abnormal spindle poles. J Cell Sci. 1988;89(Pt 1):25–38. https://doi.org/10.1242/jcs.89.1.25 PMID: 3417791
35. Kitada K, Johnson AL, Johnston LH, Sugino A. A multicopy suppressor gene of the Saccharomyces cerevisiae G1 cell cycle mutant gene dbf4 encodes a protein kinase and is identified as CDC5. Mol Cell Biol. 1993;13(7):4445–57. https://doi.org/10.1128/mcb.13.7.4445-4457.1993 PMID: 8321244

36. Ohkura H, Hagan IM, Glover DM. The conserved Schizosaccharomyces pombe kinase plo1, required to form a bipolar spindle, the actin ring, and septum, can drive septum formation in G1 and G2 cells. Genes Dev. 1995;9(9):1059–73. https://doi.org/10.1101/gad.9.9.1059 PMID: 7744248
37. Hamanaka R, Maloid S, Smith MR, O'Connell CD, Longo DL, Ferris DK. Cloning and characterization of human and murine homologues of the Drosophila polo serine-threonine kinase. Cell Growth Differ. 1994;5(3):249–57. PMID: 8018557
38. Zitouni S, Nabais C, Jana SC, Guerrero A, Bettencourt-Dias M. Polo-like kinases: structural variations lead to multiple functions. Nat Rev Mol Cell Biol. 2014;15(7):433–52. https://doi.org/10.1038/nrm3819 PMID: 24954208
39. Iliaki S, Beyaert R, Afonina IS. Polo-like kinase 1 (PLK1) signaling in cancer and beyond. Biochem Pharmacol. 2021;193:114747. https://doi.org/10.1016/j.bcp.2021.114747 PMID: 34454931
40. Long T, Cailliau K, Beckmann S, Browaeys E, Trolet J, Grevelding CG, et al. Schistosoma mansoni Polo-like kinase 1: A mitotic kinase with key functions in parasite reproduction. Int J Parasitol. 2010;40(9):1075–86. https://doi.org/10.1016/j.ijpara.2010.03.002 PMID: 20350550
41. Dissous C, Grevelding CG, Long T. Schistosoma mansoni Polo-like kinases and their function in control of mitosis and parasite reproduction. An Acad Bras Cienc. 2011;83(2):627–35. https://doi.org/10.1590/s0001-37652011000200022 PMID: 21670883
42. Long T, Neitz RJ, Beasley R, Kalyanaraman C, Suzuki BM, Jacobson MP, et al. Structure-Bioactivity Relationship for Benzimidazole Thiophene Inhibitors of Polo-Like Kinase 1 (PLK1), a Potential Drug Target in Schistosoma mansoni. PLoS Negl Trop Dis. 2016;10(1):e0004356. https://doi.org/10.1371/journal.pntd.0004356 PMID: 26751972
43. Schubert A, Koziol U, Cailliau K, Vanderstraete M, Dissous C, Brehm K. Targeting Echinococcus multilocularis stem cells by inhibition of the Polo-like kinase EmPlk1. PLoS Negl Trop Dis. 2014;8(6):e2870. https://doi.org/10.1371/journal.pntd.0002870 PMID: 24901228
44. Houhou H, Puckelwaldt O, Strube C, Haeberlein S. Reference gene analysis and its use for kinase expression profiling in *Fasciola hepatica*. Sci Rep. 2019;9(1):15867. https://doi.org/10.1038/s41598-019-52416-x PMID: 31676853
45. Morawietz CM, Houhou H, Puckelwaldt O, Hehr L, Dreisbach D, Mokosch A, et al. Targeting Kinases in *Fasciola hepatica*: Anthelminthic Effects and Tissue Distribution of Selected Kinase Inhibitors. Front Vet Sci. 2020;7:611270. https://doi.org/10.3389/fvets.2020.611270 PMID: 33409299
46. Robb E, McCammick EM, Wells D, McVeigh P, Gardiner E, Armstrong R, et al. Transcriptomic analysis supports a role for the nervous system in regulating growth and development of *Fasciola hepatica* juveniles. PLoS Negl Trop Dis. 2022;16(11):e0010854. https://doi.org/10.1371/journal.pntd.0010854 PMID: 36342907
47. Cwiklinski K, Dalton JP, Dufresne PJ, La Course J, Williams DJ, Hodgkinson J, et al. The *Fasciola hepatica* genome: gene duplication and polymorphism reveals adaptation to the host environment and the capacity for rapid evolution. Genome Biol. 2015;16(1):71. https://doi.org/10.1186/s13059-015-0632-2 PMID: 25887684
48. Plowman GD, Sudarsanam S, Bingham J, Whyte D, Hunter T. The protein kinases of Caenorhabditis elegans: a model for signal transduction in multicellular organisms. Proc Natl Acad Sci U S A. 1999;96(24):13603–10. https://doi.org/10.1073/pnas.96.24.13603 PMID: 10570119
49. Manning G, Plowman GD, Hunter T, Sudarsanam S. Evolution of protein kinase signaling from yeast to man. Trends Biochem Sci. 2002;27(10):514–20. https://doi.org/10.1016/s0968-0004(02)02179-5 PMID: 12368087
50. Skelding KA, Rostas JAP. The role of molecular regulation and targeting in regulating calcium/calmodulin stimulated protein kinases. Adv Exp Med Biol. 2012;740:703–30. https://doi.org/10.1007/978-94-007-2888-2_31 PMID: 22453966
51. You H, McManus DP, Hu W, Smout MJ, Brindley PJ, Gobert GN. Transcriptional responses of in vivo praziquantel exposure in schistosomes identifies a functional role for calcium signalling pathway member CamKII. PLoS Pathog. 2013;9(3):e1003254. https://doi.org/10.1371/journal.ppat.1003254 PMID: 23555262
52. Hirst NL, Lawton SP, Walker AJ. CaMKII regulates neuromuscular activity and survival of the human blood fluke Schistosoma mansoni. Sci Rep. 2022;12(1):19831. https://doi.org/10.1038/s41598-022-23962-8 PMID: 36400915
53. Chowdhury I, Dashi G, Keskitalo S. CMGC Kinases in Health and Cancer. Cancers (Basel). 2023;15(15):3838. https://doi.org/10.3390/cancers15153838 PMID: 37568654
54. Puckelwaldt O, Gramberg S, Ajmera S, Koepke J, Samakovlis C, Haeberlein S. Single-cell transcriptomics identifies a p21-activated kinase important for survival of the zoonotic parasite *Fasciola hepatica*. bioRxiv. 2024; 2024.03.26.586785. https://doi.org/10.1101/2024.03.26.586785
55. Kanev GK, de Graaf C, de Esch IJP, Leurs R, Würdinger T, Westerman BA, et al. The Landscape of Atypical and Eukaryotic Protein Kinases. Trends Pharmacol Sci. 2019;40(11):818–32. https://doi.org/10.1016/j.tips.2019.09.002 PMID: 31677919
56. Zaru R, Magrane M, O'Donovan C, UniProt Consortium. From the research laboratory to the database: the Caenorhabditis elegans kinome in UniProtKB. Biochem J. 2017;474(4):493–515. https://doi.org/10.1042/BCJ20160991 PMID: 28159896
57. Hua H, Kong Q, Zhang H, Wang J, Luo T, Jiang Y. Targeting mTOR for cancer therapy. J Hematol Oncol. 2019;12(1):71. https://doi.org/10.1186/s13045-019-0754-1 PMID: 31277692
58. Weber AM, Ryan AJ. ATM and ATR as therapeutic targets in cancer. Pharmacol Ther. 2015;149:124–38. https://doi.org/10.1016/j.pharmthera.2014.12.001 PMID: 25512053
59. Burke JE, Triscott J, Emerling BM, Hammond GRV. Beyond PI3Ks: targeting phosphoinositide kinases in disease. Nat Rev Drug Discov. 2023;22(5):357–86. https://doi.org/10.1038/s41573-022-00582-5 PMID: 36376561
60. Malumbres M, Barbacid M. Cell cycle, CDKs and cancer: a changing paradigm. Nat Rev Cancer. 2009;9(3):153–66. https://doi.org/10.1038/nrc2602 PMID: 19238148

61. Wang XQ, Lo CM, Chen L, Ngan ES-W, Xu A, Poon RY. CDK1-PDK1-PI3K/Akt signaling pathway regulates embryonic and induced pluripotency. Cell Death Differ. 2017;24(1):38–48. https://doi.org/10.1038/cdd.2016.84 PMID: 27636107
62. Santamaría D, Barrière C, Cerqueira A, Hunt S, Tardy C, Newton K, et al. Cdk1 is sufficient to drive the mammalian cell cycle. Nature. 2007;448(7155):811–5. https://doi.org/10.1038/nature06046 PMID: 17700700
63. Babina IS, Turner NC. Advances and challenges in targeting FGFR signalling in cancer. Nat Rev Cancer. 2017;17(5):318–32. https://doi.org/10.1038/nrc.2017.8 PMID: 28303906
64. Förster S, Koziol U, Schäfer T, Duvoisin R, Cailliau K, Vanderstraete M, et al. The role of fibroblast growth factor signalling in Echinococcus multilocularis development and host-parasite interaction. PLoS Negl Trop Dis. 2019;13(3):e0006959. https://doi.org/10.1371/journal.pntd.0006959 PMID: 30849083
65. Du X, McManus DP, French JD, Collinson N, Sivakumaran H, MacGregor SR, et al. CRISPR interference for sequence-specific regulation of fibroblast growth factor receptor A in Schistosoma mansoni. Front Immunol. 2023;13:1105719. https://doi.org/10.3389/fimmu.2022.1105719 PMID: 36713455
66. Roskoski R Jr. Properties of FDA-approved small molecule protein kinase inhibitors: A 2021 update. Pharmacol Res. 2021;165:105463. https://doi.org/10.1016/j.phrs.2021.105463 PMID: 33513356
67. Strebhardt K, Ullrich A. Targeting polo-like kinase 1 for cancer therapy. Nat Rev Cancer. 2006;6(4):321–30. https://doi.org/10.1038/nrc1841 PMID: 16557283
68. Hanks SK, Hunter T. The eukaryotic protein kinase superfamily: kinase (catalytic) domain structure and classification 1. The FASEB Journal. 1995;9(8):576–96. https://doi.org/10.1096/fasebj.9.8.7768349
69. Seki A, Coppinger JA, Jang C-Y, Yates JR, Fang G. Bora and the kinase Aurora a cooperatively activate the kinase Plk1 and control mitotic entry. Science. 2008;320(5883):1655–8. https://doi.org/10.1126/science.1157425 PMID: 18566290
70. Elia AEH, Cantley LC, Yaffe MB. Proteomic screen finds pSer/pThr-binding domain localizing Plk1 to mitotic substrates. Science. 2003;299(5610):1228–31. https://doi.org/10.1126/science.1079079 PMID: 12595692
71. Elia AEH, Rellos P, Haire LF, Chao JW, Ivins FJ, Hoepker K, et al. The molecular basis for phosphodependent substrate targeting and regulation of Plks by the Polo-box domain. Cell. 2003;115(1):83–95. https://doi.org/10.1016/s0092-8674(03)00725-6 PMID: 14532005
72. Wang J, Chen R, Collins JJ 3rd. Systematically improved in vitro culture conditions reveal new insights into the reproductive biology of the human parasite Schistosoma mansoni. PLoS Biol. 2019;17(5):e3000254. https://doi.org/10.1371/journal.pbio.3000254 PMID: 31067225
73. Hanna R. *Fasciola hepatica*: Histology of the Reproductive Organs and Differential Effects of Triclabendazole on Drug-Sensitive and Drug-Resistant Fluke Isolates and on Flukes from Selected Field Cases. Pathogens. 2015;4(3):431–56. https://doi.org/10.3390/pathogens4030431 PMID: 26131614
74. Bjoerkman N, Thorsell W. On the ultrastructure of the ovary of the liver fluke (*Fasciola hepatica* L.). Z Zellforsch Mikrosk Anat. 1964;63:538–49. https://doi.org/10.1007/BF00339489 PMID: 14254750
75. Marzluff WF, Wagner EJ, Duronio RJ. Metabolism and regulation of canonical histone mRNAs: life without a poly(A) tail. Nat Rev Genet. 2008;9(11):843–54. https://doi.org/10.1038/nrg2438 PMID: 18927579
76. Solana J, Kao D, Mihaylova Y, Jaber-Hijazi F, Malla S, Wilson R, et al. Defining the molecular profile of planarian pluripotent stem cells using a combinatorial RNAseq, RNA interference and irradiation approach. Genome Biol. 2012;13(3):R19. https://doi.org/10.1186/gb-2012-13-3-r19 PMID: 22439894
77. Spänkuch-Schmitt B, Bereiter-Hahn J, Kaufmann M, Strebhardt K. Effect of RNA silencing of polo-like kinase-1 (PLK1) on apoptosis and spindle formation in human cancer cells. J Natl Cancer Inst. 2002;94(24):1863–77. https://doi.org/10.1093/jnci/94.24.1863 PMID: 12488480
78. McCarroll JA, Dwarte T, Baigude H, Dang J, Yang L, Erlich RB, et al. Therapeutic targeting of polo-like kinase 1 using RNA-interfering nanoparticles (iNOPs) for the treatment of non-small cell lung cancer. Oncotarget. 2015;6(14):12020–34. https://doi.org/10.18632/oncotarget.2664 PMID: 25557168
79. Herz M, Zarowiecki M, Wessels L, Pätzel K, Herrmann R, Braun C, et al. Genome-wide transcriptome analysis of Echinococcus multilocularis larvae and germinative cell cultures reveals genes involved in parasite stem cell function. Front Cell Infect Microbiol. 2024;14:1335946. https://doi.org/10.3389/fcimb.2024.1335946 PMID: 38333034
80. Sampath P, Pritchard DK, Pabon L, Reinecke H, Schwartz SM, Morris DR, et al. A hierarchical network controls protein translation during murine embryonic stem cell self-renewal and differentiation. Cell Stem Cell. 2008;2(5):448–60. https://doi.org/10.1016/j.stem.2008.03.013 PMID: 18462695
81. Saba JA, Liakath-Ali K, Green R, Watt FM. Translational control of stem cell function. Nat Rev Mol Cell Biol. 2021;22(10):671–90. https://doi.org/10.1038/s41580-021-00386-2 PMID: 34272502
82. Larson DE, Xie W, Glibetic M, O'Mahony D, Sells BH, Rothblum LI. Coordinated decreases in rRNA gene transcription factors and rRNA synthesis during muscle cell differentiation. Proc Natl Acad Sci U S A. 1993;90(17):7933–6. https://doi.org/10.1073/pnas.90.17.7933 PMID: 8396256
83. Cong Y, Yang H, Zhang P, Xie Y, Cao X, Zhang L. Transcriptome Analysis of the Nematode Caenorhabditis elegans in Acidic Stress Environments. Front Physiol. 2020;11:1107. https://doi.org/10.3389/fphys.2020.01107 PMID: 33013473

84. Jasmer DP, Rosa BA, Mitreva M. Cell Death and Transcriptional Responses Induced in Larvae of the Nematode Haemonchus contortus by Toxins/Toxicants with Broad Phylogenetic Efficacy. Pharmaceuticals (Basel). 2021;14(7):598. https://doi.org/10.3390/ph14070598 PMID: 34206464
85. Chen J. The Cell-Cycle Arrest and Apoptotic Functions of p53 in Tumor Initiation and Progression. Cold Spring Harb Perspect Med. 2016;6(3):a026104. https://doi.org/10.1101/cshperspect.a026104 PMID: 26931810
86. Duffy MJ, Synnott NC, Crown J. Mutant p53 as a target for cancer treatment. Eur J Cancer. 2017;83:258–65. https://doi.org/10.1016/j.ejca.2017.06.023 PMID: 28756138
87. Fei L, Xu H. Role of MCM2-7 protein phosphorylation in human cancer cells. Cell Biosci. 2018;8:43. https://doi.org/10.1186/s13578-018-0242-2 PMID: 30062004
88. McCusker P, Hussain W, McVeigh P, McCammick E, Clarke NG, Robb E, et al. RNA interference dynamics in juvenile *Fasciola hepatica* are altered during in vitro growth and development. Int J Parasitol Drugs Drug Resist. 2020;14:46–55. https://doi.org/10.1016/j.ijpddr.2020.08.004 PMID: 32866764
89. Vigneron S, Brioudes E, Burgess A, Labbé J-C, Lorca T, Castro A. Greatwall maintains mitosis through regulation of PP2A. EMBO J. 2009;28(18):2786–93. https://doi.org/10.1038/emboj.2009.228 PMID: 19680222
90. Im J-S, Ki S-H, Farina A, Jung D-S, Hurwitz J, Lee J-K. Assembly of the Cdc45-Mcm2-7-GINS complex in human cells requires the Ctf4/And-1, RecQL4, and Mcm10 proteins. Proc Natl Acad Sci U S A. 2009;106(37):15628–32. https://doi.org/10.1073/pnas.0908039106 PMID: 19805216
91. Komorowska K, Doyle A, Wahlestedt M, Subramaniam A, Debnath S, Chen J, et al. Hepatic Leukemia Factor Maintains Quiescence of Hematopoietic Stem Cells and Protects the Stem Cell Pool during Regeneration. Cell Rep. 2017;21(12):3514–23. https://doi.org/10.1016/j.celrep.2017.11.084 PMID: 29262330
92. Stoll K, Bergmann M, Spiliotis M, Brehm K. A MEKK1 - JNK mitogen activated kinase (MAPK) cascade module is active in Echinococcus multilocularis stem cells. PLoS Negl Trop Dis. 2021;15(12):e0010027. https://doi.org/10.1371/journal.pntd.0010027 PMID: 34879059
93. Beyer EC, Berthoud VM. Gap junction gene and protein families: Connexins, innexins, and pannexins. Biochim Biophys Acta Biomembr. 2018;1860(1):5–8. https://doi.org/10.1016/j.bbamem.2017.05.016 PMID: 28559187
94. Settles SE, Miller KE, Roberts-Galbraith RH. A parenchymal niche regulates pluripotent stem cell function in planarians. bioRxiv. 2025;:2025.08.01.668211. https://doi.org/10.1101/2025.08.01.668211 PMID: 40766428
95. Nogi T, Levin M. Characterization of innexin gene expression and functional roles of gap-junctional communication in planarian regeneration. Dev Biol. 2005;287(2):314–35. https://doi.org/10.1016/j.ydbio.2005.09.002 PMID: 16243308
96. Oviedo NJ, Morokuma J, Walentek P, Kema IP, Gu MB, Ahn J-M, et al. Long-range neural and gap junction protein-mediated cues control polarity during planarian regeneration. Dev Biol. 2010;339(1):188–99. https://doi.org/10.1016/j.ydbio.2009.12.012 PMID: 20026026
97. Oviedo NJ, Levin M. smedinx-11 is a planarian stem cell gap junction gene required for regeneration and homeostasis. Development. 2007;134(17):3121–31. https://doi.org/10.1242/dev.006635 PMID: 17670787
98. Maule AG, Marks NJ, Day TA. Signalling molecules and nerve-muscle function. In: Maule AG, Marks N, editors. Parasitic flatworms: Molecular biology, biochemistry, immunology and physiology. CABI. 2006. p. 369–81.
99. El-Shehabi F, Ribeiro P. Histamine signalling in Schistosoma mansoni: immunolocalisation and characterisation of a new histamine-responsive receptor (SmGPR-2). Int J Parasitol. 2010;40(12):1395–406. https://doi.org/10.1016/j.ijpara.2010.04.006 PMID: 20430030
100. Sukhdeo SC, Sangster NC, Mettrick DF. Effects of Cholinergic Drugs on Longitudinal Muscle Contractions of *Fasciola hepatica*. J Parasitol. 1986;72(6):858. https://doi.org/10.2307/3281834
101. Sukhdeo MVK, Mettrick DF. The Behavior of Juvenile *Fasciola hepatica*. J Parasitol. 1986;72(4):492. https://doi.org/10.2307/3281496
102. Fanburg BL, Lee SL. A new role for an old molecule: serotonin as a mitogen. Am J Physiol. 1997;272(5 Pt 1):L795-806. https://doi.org/10.1152/ajplung.1997.272.5.L795 PMID: 9176241
103. Franquinet R, Martelly I. Effects of serotonin and catecholamines on RNA synthesis in planarians; in vitro and in vivo studies. Cell Differ. 1981;10(4):201–9. https://doi.org/10.1016/0045-6039(81)90002-6 PMID: 6168391
104. Taft AS, Norante FA, Yoshino TP. The identification of inhibitors of Schistosoma mansoni miracidial transformation by incorporating a medium-throughput small-molecule screen. Exp Parasitol. 2010;125(2):84–94. https://doi.org/10.1016/j.exppara.2009.12.021 PMID: 20060828
105. Kawamoto F, Shozawa A, Kumada N, Kojima K. Possible roles of cAMP and Ca2+ in the regulation of miracidial transformation in Schistosoma mansoni. Parasitol Res. 1989;75(5):368–74. https://doi.org/10.1007/BF00931132 PMID: 2542928
106. Boyle JP, Zaide JV, Yoshino TP. Schistosoma mansoni: effects of serotonin and serotonin receptor antagonists on motility and length of primary sporocysts in vitro. Exp Parasitol. 2000;94(4):217–26. https://doi.org/10.1006/expr.2000.4500 PMID: 10831389
107. Herz M, Brehm K. Serotonin stimulates Echinococcus multilocularis larval development. Parasit Vectors. 2021;14(1):14. https://doi.org/10.1186/s13071-020-04533-0 PMID: 33407815
108. Alqahtani S, Butcher MC, Ramage G, Dalby MJ, McLean W, Nile CJ. Acetylcholine Receptors in Mesenchymal Stem Cells. Stem Cells Dev. 2023;32(3–4):47–59. https://doi.org/10.1089/scd.2022.0201 PMID: 36355611
109. Basu S, Dasgupta PS. Role of dopamine in malignant tumor growth. Endocrine. 2000;12(3):237–41. https://doi.org/10.1385/ENDO:12:3:237 PMID: 10963043

110. Lee I, Knickerbocker AC, Depew CR, Martin E, Dicent J, Miller GW, et al. Effect of altered production and storage of dopamine on development and behavior in C. elegans. bioRxiv. 2023;:2023.10.07.561350. https://doi.org/10.1101/2023.10.07.561350 PMID: 37873331

111. Neckameyer WS. Multiple roles for dopamine in Drosophila development. Dev Biol. 1996;176(2):209–19. https://doi.org/10.1006/dbio.1996.0128 PMID: 8660862

112. Rand JB, Russell RL. Choline acetyltransferase-deficient mutants of the nematode Caenorhabditis elegans. Genetics. 1984;106(2):227–48. https://doi.org/10.1093/genetics/106.2.227 PMID: 6698395

113. Zachary I, Woll PJ, Rozengurt E. A role for neuropeptides in the control of cell proliferation. Dev Biol. 1987;124(2):295–308. https://doi.org/10.1016/0012-1606(87)90483-0 PMID: 2824251

114. Kreshchenko ND. Functions of flatworm neuropeptides NPF, GYIRF and FMRF in course of pharyngeal regeneration of anterior body fragments of planarian, Girardia tigrina. Acta Biol Hung. 2008;59 Suppl:199–207. https://doi.org/10.1556/ABiol.59.2008.Suppl.29 PMID: 18652393

115. Collins JJ 3rd, Hou X, Romanova EV, Lambrus BG, Miller CM, Saberi A, et al. Genome-wide analyses reveal a role for peptide hormones in planarian germline development. PLoS Biol. 2010;8(10):e1000509. https://doi.org/10.1371/journal.pbio.1000509 PMID: 20967238

116. Saberi A, Jamal A, Beets I, Schoofs L, Newmark PA. GPCRs Direct Germline Development and Somatic Gonad Function in Planarians. PLoS Biol. 2016;14(5):e1002457. https://doi.org/10.1371/journal.pbio.1002457 PMID: 27163480

117. Baguñà J, Saló E, Romero R. Effects of activators and antagonists of the neuropeptides substance P and substance K on cell proliferation in planarians. Int J Dev Biol. 1989;33(2):261–6. PMID: 2484287

118. Li X, Weth O, Haimann M, Möscheid MF, Huber TS, Grevelding CG. Rhodopsin orphan GPCR20 interacts with neuropeptides and directs growth, sexual differentiation, and egg production in female Schistosoma mansoni. Microbiol Spectr. 2024;12(1):e0219323. https://doi.org/10.1128/spectrum.02193-23 PMID: 38047698

119. Almuedo-Castillo M, Sureda-Gómez M, Adell T. Wnt signaling in planarians: new answers to old questions. Int J Dev Biol. 2012;56(1–3):53–65. https://doi.org/10.1387/ijdb.113451ma PMID: 22450995

120. Ye Z, Xu J, Feng X, Jia Y, Fu Z, Hong Y, et al. Spatiotemporal expression pattern of Sjfz7 and its expression comparison with other frizzled family genes in developmental stages of *Schistosoma japonicum*. Gene Expr Patterns. 2019;32:44–52. https://doi.org/10.1016/j.gep.2019.02.005 PMID: 30851426

121. Cheng G, Li X, Qin F, Xu R, Zhang Y, Liu J, et al. Functional analysis of the Frzb2 gene in *Schistosoma japonicum*. Vet Res. 2019;50(1):108. https://doi.org/10.1186/s13567-019-0716-1 PMID: 31829289

122. Koziol U, Jarero F, Olson PD, Brehm K. Comparative analysis of Wnt expression identifies a highly conserved developmental transition in flatworms. BMC Biol. 2016;14:10. https://doi.org/10.1186/s12915-016-0233-x PMID: 26941070

123. Gurley KA, Elliott SA, Simakov O, Schmidt HA, Holstein TW, Sánchez Alvarado A. Expression of secreted Wnt pathway components reveals unexpected complexity of the planarian amputation response. Dev Biol. 2010;347(1):24–39. https://doi.org/10.1016/j.ydbio.2010.08.007 PMID: 20707997

124. Adell T, Salò E, Boutros M, Bartscherer K. Smed-Evi/Wntless is required for beta-catenin-dependent and -independent processes during planarian regeneration. Development. 2009;136(6):905–10. https://doi.org/10.1242/dev.033761 PMID: 19211673

125. Li H-F, Wang X-B, Jin Y-P, Xia Y-X, Feng X-G, Yang J-M, et al. Wnt4, the first member of the Wnt family identified in *Schistosoma japonicum*, regulates worm development by the canonical pathway. Parasitol Res. 2010;107(4):795–805. https://doi.org/10.1007/s00436-010-1933-8 PMID: 20574838

126. Kobayashi C, Saito Y, Ogawa K, Agata K. Wnt signaling is required for antero-posterior patterning of the planarian brain. Dev Biol. 2007;306(2):714–24. https://doi.org/10.1016/j.ydbio.2007.04.010 PMID: 17498685

127. Armstrong R, Marks NJ, Geary TG, Harrington J, Selzer PM, Maule AG. Wnt/β-catenin signalling underpins juvenile *Fasciola hepatica* growth and development. PLoS Pathog. 2025;21(2):e1012562. https://doi.org/10.1371/journal.ppat.1012562 PMID: 39919127

128. Lingueglia E, Champigny G, Lazdunski M, Barbry P. Cloning of the amiloride-sensitive FMRFamide peptide-gated sodium channel. Nature. 1995;378(6558):730–3. https://doi.org/10.1038/378730a0 PMID: 7501021

129. Baguñà J. The planarian neoblast: the rambling history of its origin and some current black boxes. Int J Dev Biol. 2012;56(1–3):19–37. https://doi.org/10.1387/ijdb.113463jb PMID: 22252540

130. Yang D, Zhou Q, Labroska V, Qin S, Darbalaei S, Wu Y, et al. G protein-coupled receptors: structure- and function-based drug discovery. Signal Transduct Target Ther. 2021;6(1):7. https://doi.org/10.1038/s41392-020-00435-w PMID: 33414387

131. Herron CM, O'Connor A, Robb E, McCammick E, Hill C, Marks NJ, et al. Developmental Regulation and Functional Prediction of microRNAs in an Expanded *Fasciola hepatica* miRNome. Front Cell Infect Microbiol. 2022;12:811123. https://doi.org/10.3389/fcimb.2022.811123 PMID: 35223544

132. Kothe M, Kohls D, Low S, Coli R, Rennie GR, Feru F, et al. Selectivity-determining residues in Plk1. Chem Biol Drug Des. 2007;70(6):540–6. https://doi.org/10.1111/j.1747-0285.2007.00594.x PMID: 18005335

133. Steegmaier M, Hoffmann M, Baum A, Lénárt P, Petronczki M, Krssák M, et al. BI 2536, a potent and selective inhibitor of polo-like kinase 1, inhibits tumor growth in vivo. Curr Biol. 2007;17(4):316–22. https://doi.org/10.1016/j.cub.2006.12.037 PMID: 17291758

134. Long T, Vanderstraete M, Cailliau K, Morel M, Lescuyer A, Gouignard N, et al. SmSak, the second Polo-like kinase of the helminth parasite Schistosoma mansoni: conserved and unexpected roles in meiosis. PLoS One. 2012;7(6):e40045. https://doi.org/10.1371/journal.pone.0040045 PMID: 22768216

135. Bennett CE. Surface features, sensory structures, and movement of the newly excysted juvenile *Fasciola hepatica* L. J Parasitol. 1975;61(5):886–91. https://doi.org/10.2307/3279229 PMID: 1185430

136. Taylor S, Peters J-M. Polo and Aurora kinases: lessons derived from chemical biology. Curr Opin Cell Biol. 2008;20(1):77–84. https://doi.org/10.1016/j.ceb.2007.11.008 PMID: 18249108

137. Gelmedin V, Dissous C, Grevelding CG. Re-positioning protein-kinase inhibitors against schistosomiasis. Future Med Chem. 2015;7(6):737–52. https://doi.org/10.4155/fmc.15.31 PMID: 25996067

138. McNulty SN, Tort JF, Rinaldi G, Fischer K, Rosa BA, Smircich P, et al. Genomes of *Fasciola hepatica* from the Americas Reveal Colonization with Neorickettsia Endobacteria Related to the Agents of Potomac Horse and Human Sennetsu Fevers. PLoS Genet. 2017;13(1):e1006537. https://doi.org/10.1371/journal.pgen.1006537 PMID: 28060841

139. Lee RYN, Howe KL, Harris TW, Arnaboldi V, Cain S, Chan J, et al. WormBase 2017: molting into a new stage. Nucleic Acids Res. 2018;46(D1):D869–74. https://doi.org/10.1093/nar/gkx998 PMID: 29069413

140. Frickey T, Lupas A. CLANS: a Java application for visualizing protein families based on pairwise similarity. Bioinformatics. 2004;20(18):3702–4. https://doi.org/10.1093/bioinformatics/bth444 PMID: 15284097

141. Tamura K, Stecher G, Kumar S. MEGA11: Molecular Evolutionary Genetics Analysis Version 11. Mol Biol Evol. 2021;38(7):3022–7. https://doi.org/10.1093/molbev/msab120 PMID: 33892491

142. McVeigh P, McCammick EM, McCusker P, Morphew RM, Mousley A, Abidi A, et al. RNAi dynamics in Juvenile Fasciola spp. Liver flukes reveals the persistence of gene silencing in vitro. PLoS Negl Trop Dis. 2014;8(9):e3185. https://doi.org/10.1371/journal.pntd.0003185 PMID: 25254508

143. Untergasser A, Nijveen H, Rao X, Bisseling T, Geurts R, Leunissen JAM. Primer3Plus, an enhanced web interface to Primer3. Nucleic Acids Res. 2007;35(Web Server issue):W71-4. https://doi.org/10.1093/nar/gkm306 PMID: 17485472

144. Schneider CA, Rasband WS, Eliceiri KW. NIH Image to ImageJ: 25 years of image analysis. Nat Methods. 2012;9(7):671–5. https://doi.org/10.1038/nmeth.2089 PMID: 22930834

145. Pfaffl MW. A new mathematical model for relative quantification in real-time RT-PCR. Nucleic Acids Res. 2001;29(9):e45. https://doi.org/10.1093/nar/29.9.e45 PMID: 11328886

146. Götz S, García-Gómez JM, Terol J, Williams TD, Nagaraj SH, Nueda MJ, et al. High-throughput functional annotation and data mining with the Blast2GO suite. Nucleic Acids Res. 2008;36(10):3420–35. https://doi.org/10.1093/nar/gkn176 PMID: 18445632

147. Cantalapiedra CP, Hernández-Plaza A, Letunic I, Bork P, Huerta-Cepas J. eggNOG-mapper v2: Functional Annotation, Orthology Assignments, and Domain Prediction at the Metagenomic Scale. Mol Biol Evol. 2021;38(12):5825–9. https://doi.org/10.1093/molbev/msab293 PMID: 34597405

148. Gillan V, Maitland K, Laing R, Gu H, Marks ND, Winter AD, et al. Increased Expression of a MicroRNA Correlates with Anthelmintic Resistance in Parasitic Nematodes. Front Cell Infect Microbiol. 2017;7:452. https://doi.org/10.3389/fcimb.2017.00452 PMID: 29209592